ISTANBUL TECHNICAL UNIVERSITY ★ GRADUATE SCHOOL OF SCIENCE ENGINEERING AND TECHNOLOGY

SIMULATION OF THE CLUTCH HILL START TEST FOR HEAVY COMMERCIAL VEHICLES

M.Sc. THESIS

Cem ERBAŞ

Department of Aeronautics and Astronautics Engineering

Interdisciplinary Program

FEBRUARY 2015

ISTANBUL TECHNICAL UNIVERSITY ★ GRADUATE SCHOOL OF SCIENCE ENGINEERING AND TECHNOLOGY

SIMULATION OF THE CLUTCH HILL START TEST FOR HEAVY COMMERCIAL VEHICLES

M.Sc. THESIS

Cem ERBAŞ
(511101106)

Department of Aeronautics and Astronautics Engineering

Interdisciplinary Program

Thesis Advisor: Prof. Vedat Ziya DOĞAN

FEBRUARY 2015

İSTANBUL TEKNİK ÜNİVERSİTESİ ★ FEN BİLİMLERİ ENSTİTÜSÜ

AĞIR TİCARİ ARAÇLARDA DEBRİYAJ YOKUŞ KALKIŞ TESTİNİN SİMÜLASYONU

YÜKSEK LİSANS TEZİ

Cem ERBAŞ
(511101106)

Uçak ve Uzay Mühendisliği

Disiplinlerarası Program

Tez Danışmanı: Prof. Dr. Vedat Ziya DOĞAN

ŞUBAT 2015

Cem ERBAŞ, a **M.Sc.** student of ITU **Graduate School of Science Engineering and Technology, Department of Aeronautics and Astronautics Engineering,** student ID **511101106** successfully defended the **thesis** entitled **"Simulation of the Clutch Hill Start Test for Heavy Commercial Vehicles"**, which he prepared after fulfilling the requirements specified in the associated legislations, before the jury whose signatures are below.

Thesis Advisor :	**Prof. Vedat Ziya DOĞAN** İstanbul Technical University	.....
Jury Members :	**Prof. Zahit MECİTOĞLU** Istanbul Technical University	.....
	Prof. Ata MUĞAN Istanbul Technical University	.....

Date of Submission : 11 December 2014
Date of Defense : 23 January 2015

Dedicated to my family,

FOREWORD

First of all, I appreciate my Professor, Vedat Ziya Doğan, for his great knowledge, academic experience, guidance and understanding, which he has provided to me throughout my master of science thesis.

I also would like to thank my Supervisor at Ford Motor Company, Çağkan Kocabaş, for providing me his continuous support, and for looking from different perspectives to support me in completing this study.

Further, plenty of thanks to my family for always being with me in my life. Their confidence in me is one of the key factors for my motivation.

Finally, thanks to everyone else who has given their contributions to the study.

February 2015

Cem ERBAŞ
Mechanical Engineer

TABLE OF CONTENTS

Page

ABBREVIATIONS

DCOV	**:** Define, Characterize, Optimize, Verify
DMAIC	**:** Define, Measure, Analyse, Improve, Control
DOE	**:** Design of Experiment
FDR	**:** Final Drive Ratio
GVM	**:** Gross Vehicle Mass
GTM	**:** Gross Total Mass
OEM	**:** Original Equipment Manufacturers
R^2	**:** Coefficient of Determination

LIST OF TABLES

Page

LIST OF FIGURES

Page

SIMULATION OF THE CLUTCH HILL START TEST FOR HEAVY COMMERCIAL VEHICLES

SUMMARY

Clutch hill start test is one of the most critical and specific vehicle tests for validating the clutch system. It helps us to understand the thermal capability of the clutch during repetitive vehicle operation.

During the vehicle launch, the kinetic energy in the clutch is converted to heat with respect to the first law of thermodynamics. The heat dissipation takes place by conduction between the clutch's frictional components, while it takes place by convection to the environment. The components of the clutch are heated due to this process. The clutch must be capable of dissipating the heat throughout the assembly in order to cool itself down. If the clutch is exposed to extreme heat, it may potentially cease to function due to thermal destruction.

The amount of dissipated heat energy in the clutch depends highly on several vehicle properties such as the transmission gear ratio, final drive ratio (FDR), tire size and vehicle mass. It also depends on the driver's operating behavior, namely, the duration of the gas and clutch pedal inflection.

Before the test, thermocouples are installed inside the clutch housing, which houses the clutch mechanism and instrumentations. During the test, the temperature of the air within the clutch housing is measured to see if the clutch passes the test and operates within acceptable temperature limits.

In the procedure defined by the Ford Motor Company, the test is performed with a fully loaded vehicle, on a road with a 10% slope. The driveline properties are selected to ensure that the wheel traction force is minimum so that the slip time and the heat dissipation in the clutch is maximum. The test begins when the air temperature inside the clutch housing is 80° celsius. The driver shifts the gear from neutral, moves the vehicle by depressing the gas pedal and releasing the clutch pedal, then stops, and waits for 60 seconds. This cycle is repeated 100 times. Temperatures are observed at each step of the test and final temperatures are evaluated whether the test is successfully passed.

In this thesis, the simulation of clutch hill start test has been established. This type of simulation has not been available within the Ford Motor Company. It has been built on GT-SUITE commercial software. Not only has the entire driveline been created, but also a model for the driver. Furthermore, a thermal section has been created and optimized for heavy commercial vehicles. In the simulation, the driver changes the gears (first gear), drives the vehicle at a certain speed, stops it, and waits for 60 seconds. Then runs the vehicle again. The air temperature within the clutch housing is determined at the end of the simulation The simulation works in correlation with vehicle tests. The results have also been compared with recorded data from three physical vehicle tests.

AĞIR TİCARİ ARAÇLARDA DEBRİYAJ YOKUŞ KALKIŞ TESTİNİN SİMÜLASYONU

ÖZET

Debriyaj, içten yanmalı motorlarda motor ile şanzıman arasında bulunan ve motordan şanzımana aktarılan tork miktarını düzenleyen bir aktarma organıdır. Gerektiğinde tork iletiminin kesilmesine yardımcı olmakta ve vites değiştirilebilmesini sağlamaktadır. Aktarılan tork miktarını ayarlayabilmesinin yanısıra, içten yanmalı motorların silindirlerinde yanmadan dolayı oluşan titreşimleri üzerinde bulunan damper yaylarıyla filtreleyip sönümlediği için için konfor açısından da çok önemli bir sistemdir. Debriyaj sistemi, krank miline bağlı volan ve volana bağlı debriyaj baskı komplesi arasında şanzıman prizdirek mili üzerindeki debriyaj balatasından, baskı komplesine bağlı ayırma rulmanından ve ayırma-kavramayı gerçekleştiren hidrolik ayırma sisteminden oluşmaktadır. Sürücü debriyaj pedalına bastığında baskı komplesinin yaylarına bağlı ayırma rulmanı, pedala bağlı hidrolik sistem vasıtasyla baskı yaylarını hareket ettirir, debriyaj balatası üzerindeki baskı kuvveti ortadan kaybolur ve ayırma gerçekleşir. Debriyaj ayırma konumundayken, yani vites değiştirilmeden hemen once krank mili ve şanzıman prizdirek milleri farklı hızlarda dönmektedir. Sürücü vitesi değiştirip ayağını debriyaj pedalından kaldırdığı zaman kavrama başlar ve tekerleklere tork aktarımı gerçekleşir. Hız farkı sıfırlandığında ise kavrama tamamlanır.

Geçmişten günümüze kadar birçok debriyaj çeşidi kullanılmıştır. Bunlardan ilk kullanılanlardanı ve günümüz sürtünmeli tip debriyajın atası olarak kabul edilen konik tip debriyajdır. Bu debriyaj çeşidi basit bir tasarıma sahip olmasının avantajıyla ve yapılan iyileştirmelerle 1920'lerde yaygın olarak kullanılmıştır. Ancak yapılan iyileştirmelere rağmen balata sürtünme malzemesinin kolay aşınması ve parçalarının değitirilmesinin zaman alması nedeniyle kullanımı sona ermiştir. Aynı dönemlerde Profesör Hele-Shaw çok yüzeyli debriyaj üzerinde çalışmaktaydı. Hele-Shaw çeşidi debriyajın avantajları daha geniş bir baskı yüzey alanına sahip olması ve montaj için daha az yer tutmasıydı. Dezavantajı ise ayrılma gerçekleşmesine rağmen tam tork transferinin kesilmemesi, buna bağlı olarak şanzıman dişlilerinin zarar görme olasılığının yüksek olmasıydı. Bu dezavantajından dolayı Hele-Shaw debriyaj çeşidi fazla kullanım alanına sahip olamamıştır.

1920'lerden itibaren günümüze kadar tek balatalı kuru tip debriyajın kullanımı yaygınlaşmıştır. Özellikle asbestosun bulunmasından sonra en çok kullanılan debriyaj çeşidi olmuştur. Bu sistemde vites geçişleri çok kolaydı ve kullanılan balata ağırlığı daha azdı. Tork iletimini iletmede helisel yaylar kullanılmaktaydı. Otomotiv endüstrisindeki hızlı gelişim sonucunda daha yüksek devirlere çıkan güçlü motorlar üretilmekteydi. Helisel yayların yüksek devirlerde merkezkaç kuvvetinin etkisiyle baskı kuvvetindeki değişikliklerin çok olması nedeniyle çözüm olarak diyafram yaylar kullanılmaya başlanmıştır. Modern araçlarda kullanılan debriyajlarda diyafram yay kullanılmaktadır.

Kuru tip debriyajın temel olarak iki çeşidi vardır: Çekme tip ve itme tip. Çekme tip debriyajda tork iletiminin kesilmesi diyafram yaylarının şanzıman tarafına doğru çekilmesi; İtme tip debriyajda ise motor tarafına doğru itilmesi vasıtasıyla gerçekleşir. Çekme tip debriyaj genel olarak yüksek torka sahip ticari araçlarda kullanılır. Yüksek baskı kuvvetine ve tork kapasitesine sahip olması çekme tip debriyajın başlıca avantajıdır. Dezavantajı ise daha kompleks ayırma rulmanı tasarımı ve montajının karmaşık olmasıdır. İtme tip debriyajın avantajları montajının kolay ve parçalarının basit olmasıdır. Fakat tork kapasitesi nispeten düşük olduğundan torku yüksek araçlarda itme tip debriyajın kullanılması tavsiye edilmez. Bu nedenlerden dolayı kamyon uygulamalarında genellikle çekme tip debriyaj kullanılır.

Kavrama devam ederken volan ile baskı komplesine bağlı baskı plakası arasındaki debriyaj balatası arasında sürtünme nedeniyle ısı enerjisi meydana gelir. Araç durgun halde hareketine başladığı sırada atalet maksimum olduğu için ilk kalkışta meydana gelen ısı en fazladır. Açığa çıkan ısı enerjisi debriyaj sistemi parçalarını ısıtır. Sürtünme esnasında iletilen ısı malzeme özelliklerine bağlı olarak parçalara belli oranlarda yayılmaktadır. Sıcaklık artışı, debriyajın sürtünen parçaları arasında, yani volan, debriyaj balatası ve baskı plakası arasında iletim yoluyla; çevredeki parçalara ise taşınım yoluyla iletilmektedir. Debriyajın düzgün çalışabilmesi için açığa çıkan ısıyı üzerinden atabilmesi ve soğuması gerekmektedir. Nispeten dar bir sıcaklık aralığında balata malzemesinin performansı yeterli olmasına ragmen belli bir sıcaklıktan sonra hızla düşmektedir. Dolayısıyla debriyaj balatası yüksek sıcaklık nedeniyle yanabilir ve hatta diğer metalik parçalarda bu nedenle termal çatlaklar oluşabilir. Bu durumda debriyaj sisteminin çalışması imkansız hale gelir.

Açığa çıkan ısı miktarı birçok parametreye bağlıdır. Bu parametrelerden araca bağlı olanlardan bazılarına şanzıman dişli oranı, diferansiyel son dişli oranı, tekerlek çapı ve aracın kütlesi örnek gösterilebilir. Ayrıca sürücünün aracı kullanım şekli, yani gaz ve debriyaj pedalını nasıl kullandığı da çıkan enerji miktarını değiştirmektedir.

Debriyajın sıcaklığa karşı performansı konusu mühendislerin sürekli ilgi odağı olmayı başarmış ve performansını arttırmak için geçmişten günümüze birçok araştırma yapılmaktadır. Hem sürücüye hem de araç özelliklerine bağlı olduğu için sistem validasyonunda gerek bilgisayar ortamında simülasyonlar gerek çeşitli parça ve araç testleri yapılmaktadır. Parça testleri debriyaj imalatçıları tarafından tezgahlarda yapılırken araç testleri genellikle otomotiv ana sanayi tarafından yapılmaktadır. Çalışma sırasında maruz kaldığı yüksek ısı etkisi nedeniyle en çok zorlanan güç aktarma organlarından biri olduğu için bu araç testlerinin başında debriyaj yokuş kalkış testi gelmektedir. Debriyaj yokuş kalkış testi, hem sürücünün hem de araç özelliklerinin etkisini gösteren ve sistem validasyonu için yapılan en önemli karakteristik testlerden biridir. Periyodik kalkışa maruz araçtaki debriyajın termal kapasitesi bu test ile belirlenmektedir.

Test yapılacak aracın debriyajında kalkış esnasında oluşan ısı miktarının maksimum olabilmesi için aracın yarattığı direnç torku maksimum olacak şekilde belirlenir. Araç tam olarak yüklenir, diferansiyel son dişli oranı ve tekerlekleri prosedüre göre güncellenir. Bu durumda tekerleklere giden tork miktarı minimum olur. Ayrıca, sıcaklık ölçerler debriyaj muhafazası içerisine yerleştirilir, varsa gerekli motor kalibrasyonları yapılır ve test başlamadan önce tüm ekipmanların çalıştığından emin olunur.

Ford Motor Company tarafından belirlenen prosedüre gore, hazırlıklar tamamlandıktan sonra, debriyaj muhafaza içindeki hava sıcaklığı 80 °C'ye ulaşana kadar araç belli bir süre sürülür. Sıcaklık sensörleri 80 °C'yi gösterdiğinde test tam yüklü araçla %10'luk bir eğime sahip yolda başlar. Sürücü durgun haldeki aracın vitesini birinci vitese getirir, gaz ve debriyaj pedallarını kullanarak aracı hareket ettirir, belli bir hıza ulaştığında sonrasında aracı bekletir. 60 saniye bekledikten sonra aynı döngü 100 kez tekarlanır. Testin her basamağında debriyaj muhafazası içerisindeki hava sıcaklıkları sensörlerden okunur. Testin başarıyla tamamlanıp tamamlanmadığına test sonrasında okunan son sıcaklıkların yorumlanmasından sonra karar verilir. Test sonuçlarının yorumlanmasından sonra araç veya debriyaj değişiklik yapılması gerekebilir.

Bu çalışmada sürücüye bağlı bir test olan debriyaj yokuş kalkış testi modellenmiştir. Simülasyon, testin her aşamasındaki ve sonundaki debriyaj muhafaza sıcaklıklarını araç testlerini yapmadan hesaplayabilmek için oluşturulmuştur. Bunun yanısıra simülasyon ile riskli görülen durumlar için önlem alınması, önemli araç parametrelerinin ve debriyaj sisteminin optimize edilmesi ve testin oldukça maliyetli ve zaman alıcı olmasından dolayı test boyunca yapılan masrafların önüne geçilmesi hedeflenmektedir.

Bu testin simülasyonu şimdiye kadar Ford Motor Company'de mevcut değildi. Simülasyon, şirket bünyesinde lisanslı olarak kullanılan GT-SUITE ticari yazılımıyla oluşturulmuştur. Aracın tamamı ve yol koşulları modellenmiştir. Teste tabi tutulan araçlarda kullanılan kuru sürtünmeli tip debriyajın malzeme, ağırlık, yüzey alanı, atalet bilgileri kullanılmış, bunlara ek olarak ağır ticari araçlara özgü bir termal kısmın korelasyonu geçmişte yapılmış testlerle oluşturulmuştur. Bu araç modeli programdaki kontrol ünitesi ile birlikte birbirine bağlanmıştır. Simülasyonda sürücü test prosedürünü izlemektedir. Sürücü vitesi değiştirmekte, gaz ve debriyaj pedallarına basmakta, aracı sürmekte ve 60 saniye bekletmektedir. Simülasyon sonucunda debriyaj muhafazası içerisindeki hava sıcaklıkları hesaplanmıştır ve sonuçlar üç farklı araçtan ölçülen sonuçlar ile karşılaştırılmıştır.

Validasyondan sonra başlıca önemli araç parametrelerinin debriyaj sıcaklıklarına nicel etkisini görebilmek için GT-SUITE programında toplam 432 farklı koşulun yer aldığı deney tasarımı çalışması yapılmıştır. Deney tasarımı sonucunda debriyaj enerjilerine en çok etki eden parametreler büyüklüklerine göre belirlenmiş, sonuçlar yorumlanmış ve önerilere yer verilmiştir.

1. INTRODUCTION

The friction clutch is an essential component for the torque transmission and still the most widely used clutch type in the automotive industry. Due to its working principle, the clutch is frequently subjected to frictional heat, especially during the vehicle launch. Plenty of improvements have been implemented over time to maximize the performance of the clutch. In the meantime, the investigation of the heat energy generated during sliding has always been of interest as it is one of the biggest challenges ever faced in the advancement of automotive industry. Heat is the biggest enemy of the clutch system since it leads to a reduction in the lifecycle of the system. The performance of the clutch degrades dramatically with increasing temperature since the excessive heat damages the friction lining of the clutch and other components such as the clutch pressure plate and flywheel. Eventually, in extreme temperatures, torque transfer becomes impossible. Also, thermal cracks and permenant distortions might occur. According to the feedbacks from the customers, most of the failures in the clutch system are due to excessive heat, resulting in a fading clutch [1,2].

In order to overcome such obstacles, Original Equipment Manufacturers (OEM) and clutch manufacturers perform various vehicle and component tests from the initial design phase to the final product phase. These tests include vehicle and bench tests. Vehicle tests are performed by OEM, while individual components are validated during the bench tests performed by suppliers.

For the validation of the thermal performance of the clutch, the Ford Motor Company carries out a vehicle test called clutch hill start test. Prior to testing, the vehicle is equipped according to the lowest traction at the wheels to ensure that the resistance torque caused by the complete truck is maximum.

In this research, clutch hill start test is simulated using GT-SUITE commercial software. The complete vehicle and a driver profile are modeled. The inputs of the simulation are given in Chapter 6. The simulation results are compared with the data

obtained from three vehicle tests in Chapter 7. The parameters that effect the heat energy dissipation, and the resulting temperature increase in the clutch are analyzed. Later on, these parameters are determined with their magnitude and compared by Design of Experiment (DOE) on GT-SUITE. Discussions and conclusions are given in the final chapter.

1.1 Purpose of Thesis

The objective of this master's thesis is to develop a reliable and complete vehicle model on GT-SUITE, building a simulation of the clutch hill start test for heavy commercial vehicles with manual transmissions, which is routinely performed at Ford Motor Company. The thesis aims to optimize the parameters that heavily influence the amount of heat energy generated in the clutch during the vehicle launch.

The simulation aims to predict the clutch temperatures and any possible thermal damages that may occur in the clutch without performing the vehicle tests, and to extend the clutch system's service life by optimizing the properties of the driveline and the clutch. It also aims to provide a credible reference for product validation at Ford Motor Company.

Last but not least, the simulation tool has been created to save time and expenditures required for the preparation throughout the test.

1.2 Methodology

This project is implemented by using defined engineering methods in a structured manner and aligned with Ford Motor Company's working approach, which includes various problem solving methods such as Six Sigma DCOV and DMAIC. The project consists of the following sections:

a) Literature survey

b) Mathematical analysis

c) Testing and modelling

d) Optimization and implementation

2. CLUTCH SYSTEM

2.1 Functions of Clutch

A clutch is a mechanical device placed between the engine and the transmission. The main functions of a clutch of a motor vehicle are:

a) To allow gear shifting while the vehicle is driven.

b) To transfer the torque flow to the drivetrain.

c) To equate the speed of the engine and transmission by modulating the torque flow.

d) To make a smooth start-up possible by filtering irregularities and vibrations.

e) To permit the engine to keep on running while the vehicle is in a gear as the clutch is disengaged [1,3].

As shown in Figure 2.1, the engine and the transmission speed are syncronized during the clutch engagement process and become equal when the clutch is fully engaged.

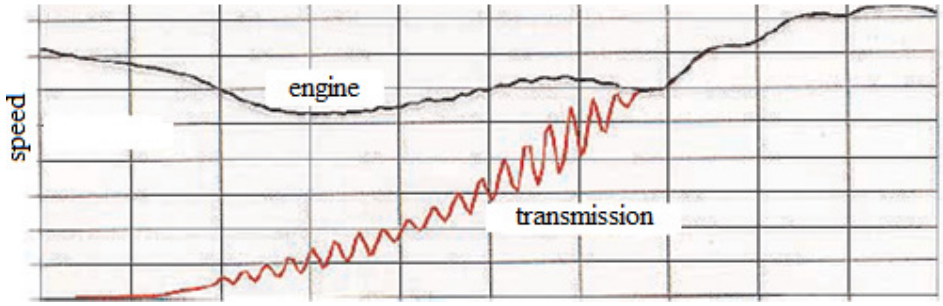

Figure 2.1 : Engine and transmission speed during the clutch engagement [4].

In principle, clutches must be designed according to the following requirements:

a) The coefficient of the friction must be as constant as possible against the temperature.

b) The heat energy generated due to the clutch slip must be dissipated efficiently.

c) The wear in the clutch must be as low as possible to extend the clutch life [5].

2.2 Operating Principle of Clutch

The clutch system operates according to the following principle:

When the driver depresses the clutch pedal, the clutch release system actuates and the clutch release bearing pushes (or pulls, depending on the clutch type) the pressure plate away from the flywheel to remove the diaphragm spring fingers' pressure from the clutch disc. This allows the clutch disc to run free and disengages the engine from the transmission. This process is illustrated for a push type clutch in Figure 2.2.

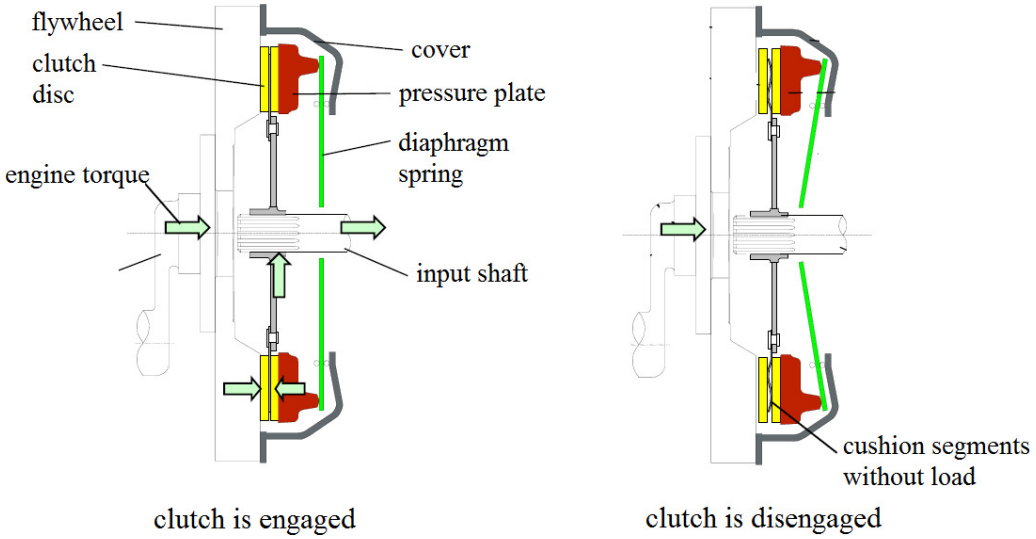

Figure 2.2 : Clutch function; engagement (left) and disengagement (right) [6].

When the driver releases the clutch pedal, the spring thrust forces the pressure plate towards the flywheel, and sandwiches the clutch disc between two surfaces [7]. Then, in the period of full engagement, the engine and transmission rotate at different speeds. Full torque transfer starts when engine and transmission rotate at the same speed.

When torque transfer is active, the clutch is considered to be engaged and the clutch disc is pressed between the engine flywheel and the clutch pressure plate. In this situation, the power that is generated in the cylinders of the engine is transferred via

the crankshaft, the flywheel and pressure plate, respectively. When torque transfer is inactive, the clutch is called disengaged, disconnecting the drive between engine and transmission, leading power flow to be cut. An overview of a complete clutch system is illustrated in Figure 2.3.

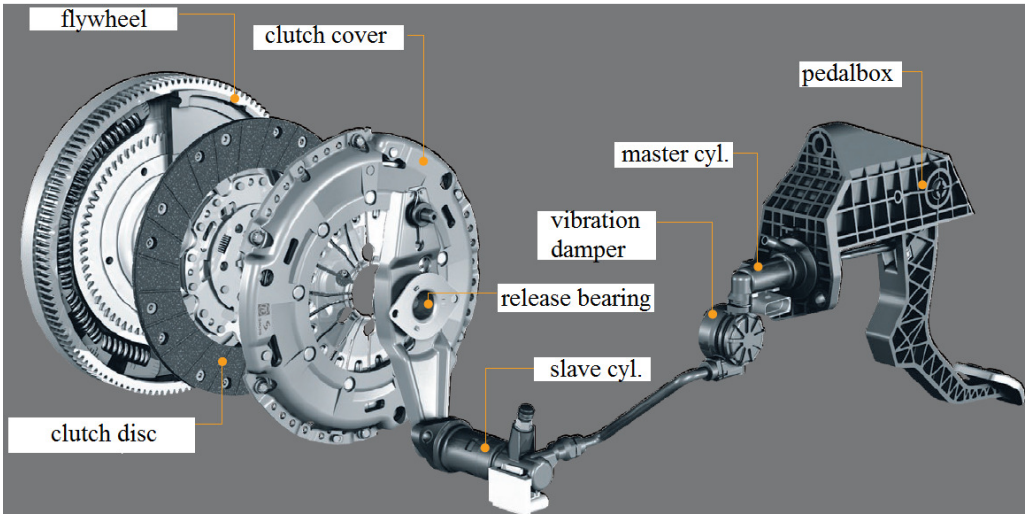

Figure 2.3 : Overview of the clutch and clutch actuation system [8].

2.3 A History of Automobile Clutch Technology

For over a century, almost every component in the automobile industry, including the clutch, has had significant developments. Driver's comfort, safety, vehicle reliability, and environmental concerns are the main criterias which inspire engineers to design better products.

Early electric and steam engines did not require clutch systems as they provided nearly constant torque. When the internal combustion engine was introduced, a division between the engine and the transmission became a necessity since its output is obtained at engine speed. The very first type of clutch for this purpose, which is actually based on our modern friction clutches, was used by Daimler in 1889. It was a cone friction clutch. The advantages included self adjusting and a simple design, which is illlustrated in Figure 2.4. On the other hand, there were a few disadvantages, namely, the friction lining used to wear out swiftly and the process for replacing it was complicated. The cone clutch has undergone numerous improvements to eliminate the disadvantages, helping it to become prevalent through the 1920s.

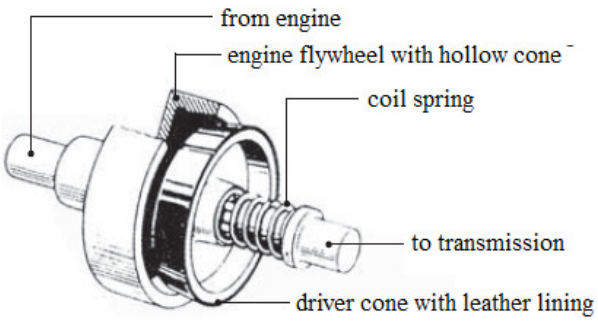

Figure 2.4 : Cross section of a cone clutch showing the typical components [9].

Professor Hele-Shaw was also developing a multi-plate clutch at the same time. Hele-Shaw's clutch had some significant advantages as it had a larger friction surface area, allowing a higher torque to transmit, and it required less space to install. Multi-plate clutches operated either immersed in oil or in a dry medium. The cross section of the Hele-Shaw's clutch is shown in Figure 2.5.

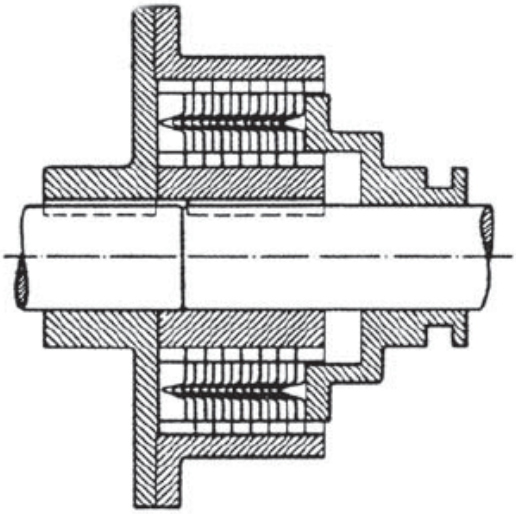

Figure 2.5 : Professor Hele-Shaw's clutch [9].

Despite its advantages, Hele Shaw's multi-plate clutch had a significant disadvantage due to the drag effect and full clutch disengagement was not possible. Thus, gear shifting operation was quite difficult and it had a tendency to damage the transmission.

Starting from the 1920s, single plate clutches began to become more common over cone and multiplate clutches, especially with the invention of asbestos linings. The single plate clutches had a relatively complicated design but great advantages over the other types available at that time. With a single plate clutch, the gear shifting was

much easier and the clutch plate had a lower mass. During this time, engineers focused on the developments for the single plate clutch. One such developement aided, the coil springs to gain acceptance. The clamp load required to transfer torque was obtained by the force of compressed coil springs. The levers compress the coil springs by a release bearing. The disadvantage of the coil spring usage was that due to the centrifugal force, the springs were forced outwards against the spring housing. This situation caused friction between the springs and the housings, resulting in a change in clamp load. The cross section of a single plate clutch showing the typical components is shown in Figure 2.6.

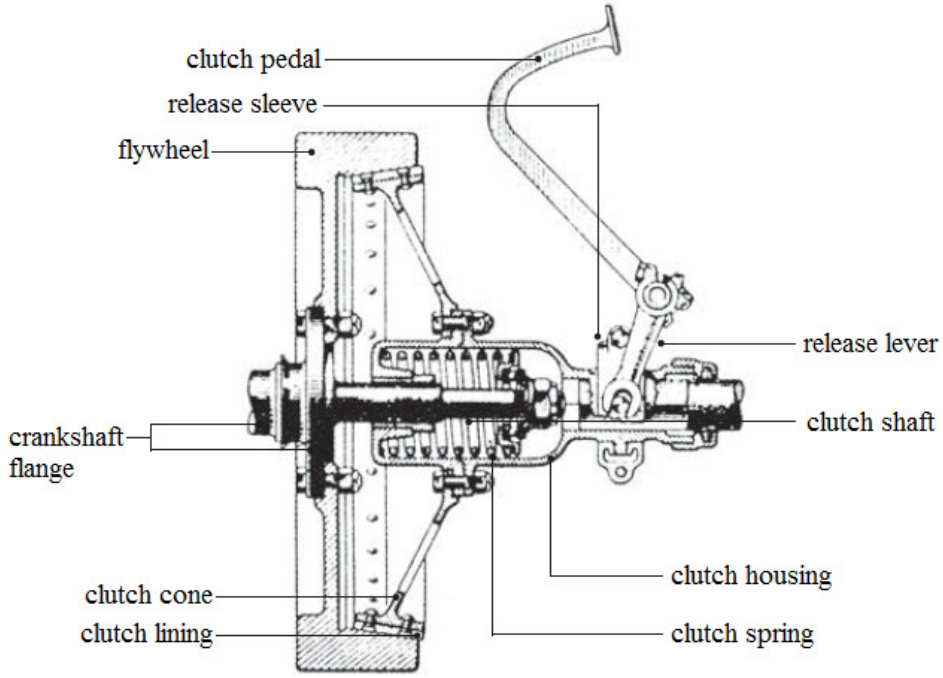

Figure 2.6 : Single plate clutch [9].

As more powerful vehicles were manufactured, diaphragm spring clutches were becoming more widely used by the end of the 1960s. The advantages of a diaphragm spring are that it provide higher and more constant clamp loads and that it takes up less space to install. Diaphragm springs are almost the only type of the spring type used nowadays.

During the diaphragm spring development, the flywheel and clutch plate were also being optimised [9].

2.4 Clutch Types

Vehicles are equipped with one of two fundamental designs of clutches, push type clutches and pull type clutches, the use of which is determined by the specifications of the powertrain and required clutch pedal loads.

2.4.1 Push type clutches

The working principle of push type clutches is that depressing the clutch pedal makes the clutch release bearing push the diaphragm spring fingers toward the engine to release the clutch. Figure 2.7 illustrates the working principle of the push type clutch.

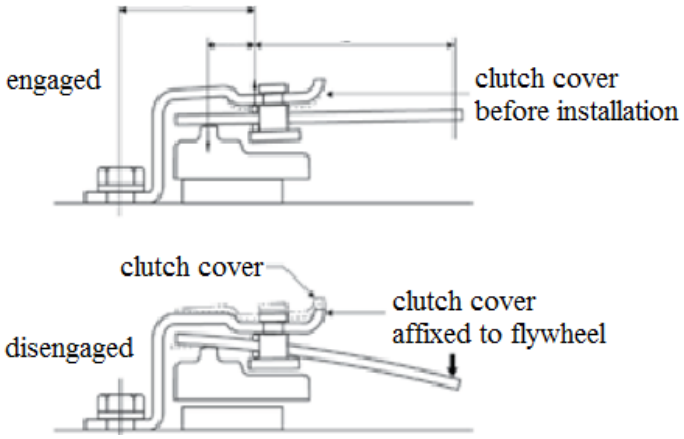

Figure 2.7 : Working principle of the push type clutch [10].

Push type clutch is the preferred design for the majority of the applications due to its easy assembly process, small installation area and simple release bearing design. An actual photo of a push type clutch is shown in Figure 2.8.

Figure 2.8 : Push type clutch [11].

2.4.2 Pull type clutches

In pull type clutches, the release bearing pulls the diaphragm fingers away from the flywheel to release the clutch. The wire ring in the clutch cover provides a pivot surface so that the pressure plate can move away from the flywheel to disengage the clutch. The working principle of the pull type clutch can be seen in Figure 2.9.

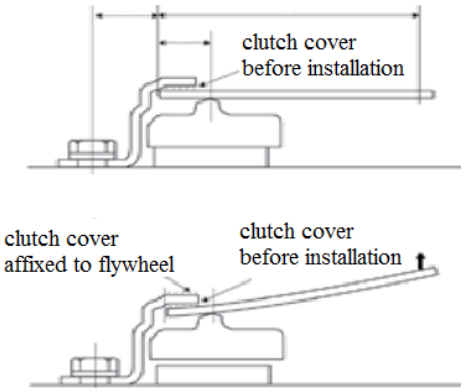

Figure 2.9 : Working principle of the pull type clutch [10].

Vehicles with high engine torque use mostly pull type clutches. The advantage is that pull type clutches maintain higher torque capacity and reduce clutch pedal loads with the aid of the clutch release fork. Also, the heat absorption of the pressure plate in the pull type clutch is more efficient as it allows a larger pressure plate to be used. Another reason why pull type clutches are used is because they can provide greater clamp load and are lighter in weight. The disadvantages of the pull type clutch are that it requires a more complex release bearing design and an installation procedure. A photo of a pull type clutch is seen in Figure 2.10.

Figure 2.10 : Pull type clutch [11].

All Ford Trucks undergone the clutch hill start test mentioned in this study had the pull type clutch.

2.5 Clutch System Components

2.5.1 Clutch disc assembly

The clutch disc assembly is the central friction element of the clutch system. The main function of the clutch disc is to transmit torque to the transmission input shaft by forming a friction system between the engine flywheel and pressure plate.

The clutch disc should have a sophisticated design such that it allows smooth startup and fast gearchanging, as well as keeping the engine vibrations away from the transmission and preventing the transmission noise as a result. It also should have as much lower inertia as possible to improve gear shift efforts and hence reduce the wear on the transmission synchronizers [12]. The clutch disc assembly consists of clutch facings, also called friction linings, which are riveted to spring segments, torsion pre/damper springs, the cushion plate, and the hub [7,9,13]. The components of a typical clutch disc are given in Figure 2.11.

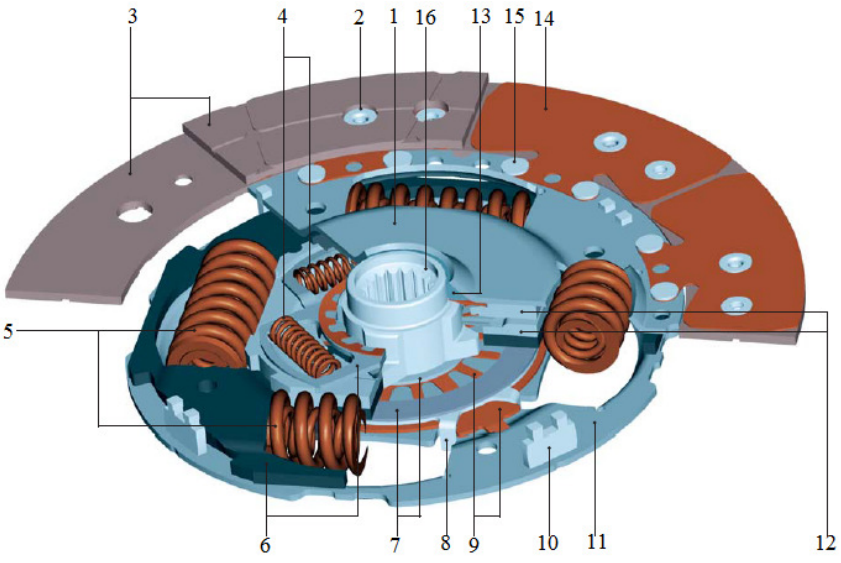

1 Drive disc
2 Friction lining rivet
3 Friction lining
4 Pressure springs (idle)
5 Pressure springs (load)
6 Hub flanges
7 Friction rings
8 Support disc
9 Diaphragm springs
10 Spacer plate
11 Mating disc
12 Damper cage assemblies
13 Centering taper
14 Axial spring cushion segment
15 Spring cushion rivet
16 Hub

Figure 2.11 : Components of the clutch disc [9].

Torsional damper springs are utilized in order to provide a smooth start and reduce torsional vibrations and irregularities generated by internal combustion engines. It has a great significance considering its duty is to optimize vibration characteristics of the powertrain [14]. As shown in Figure 2.12, the vibration levels are almost equal for the engine and transmission without torsinal damper springs, whereas they are significantly reduced at transmission side with the use of damper springs.

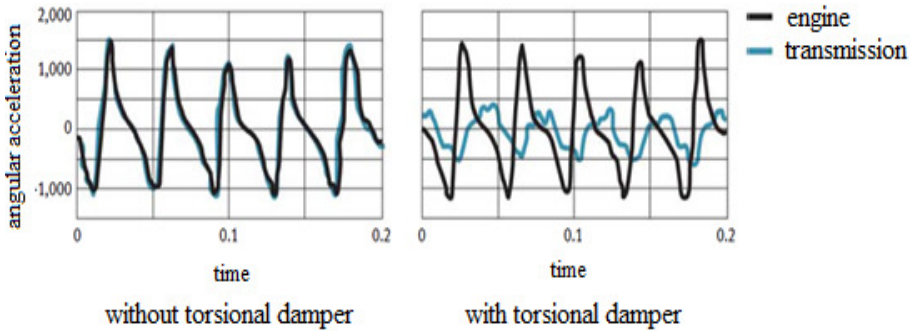

Figure 2.12 : Torsion damping effect of the damper springs [9].

In modern vehicles, clutch discs with pre-dampers and main dampers are used. Pre-dampers are comparatively low stiffness springs that are active during idle speeds, while main dampers are active as the torque transfer is in progress [16]. Their location in a clutch disc is seen in Figure 2.13.

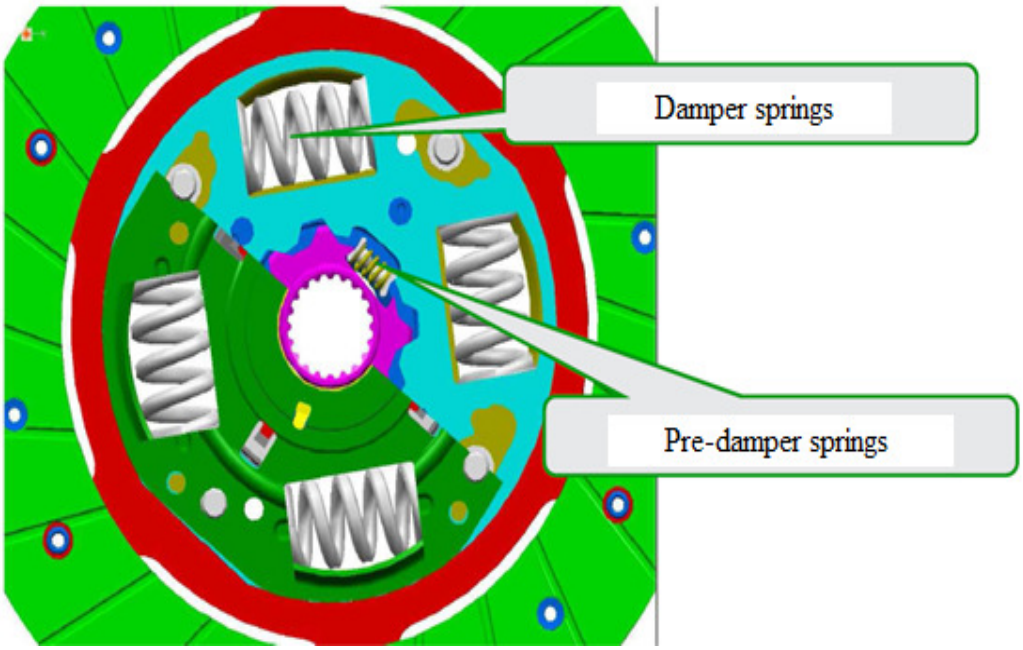

Figure 2.13 : Typical damper and predamper springs in a clutch disc [15].

In order to filter vibrations of different torque ranges, various main dampers with different stiffness values can be used. This is called a multi-stage characteristic system.

Another important part of the clutch disc assembly is friction facings which are responsible for the torque transmission. Generally, the friction facings are made of carrier thread from glass or aramide fiber and brass armature and copper, embedded in a mixture of resin and rubber [17]. The friction material must have a stuctural integrity and this is measured with the heat endurance, the clamping loads and the slip speeds of the clutch disc [22].

The heat is one of the major factors that limits the torque transmission. Depending on the usage, the clutch disc either wears out and the friction material over time or is burnt. When friction is high, which occurs specifically during clutch engagement, the temperature of the facings might increase to extremely high values quickly. In this situation, the coefficient of friction decreases in a significant manner and it is very likely to damage the base material [8,18]. In most applications where organic facing is utilized, when surface friction exceeds 300 °C the clutch starts fading with exponentially increasing damage of the material [18, 19]. Unfortunately, although plenty of studies have been performed, there is still no available friction material that has a positive gradient of friction coefficient with respect to temperature [20]. Otherwise, it would have provided a perfect torque transmission as well as fine damping characteristics [21].

The cushion spring is another significant part of the clutch disc assembly which is placed between the clutch facings and plate, shown in Figure 2.14. Together with friction facings, they account for a smooth and a gradual take up drive.

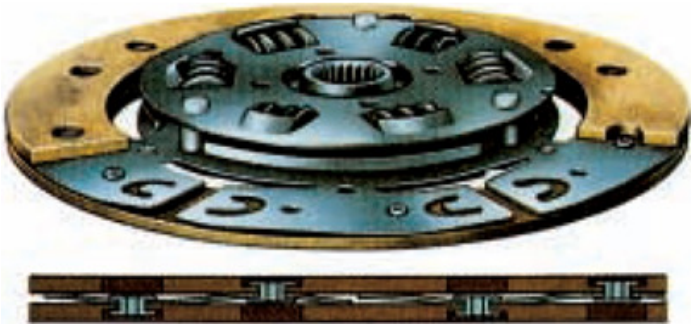

Figure 2.14 : Cushion disc [9].

During the clutch engagement, the cushion spring is pressed between the friction linings while the pressure plate pushes it against the flywheel. In return, the transmission speed can be gradually adjusted to the engine speed thanks to flexing of the cushion spring. The cushion spring also provides a good wear pattern and a uniform heat distribution as well as help reduce judder and chatter phenomena in addition to smooth startup [9]. A cushion spring's typical axial displacement with respect to clamp load can be seen in Figure 2.15.

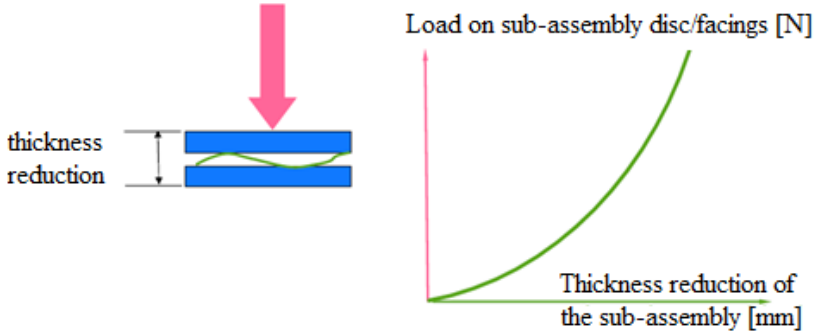

Figure 2.15 : Typical cushion disc curve [15].

2.5.2 Clutch cover assembly

Clutch cover assembly consists of a number of essential parts, that is, a pressed steel housing, a pressure plate with a machined flat surface, diaphragm spring, a number of tangential leaf springs and wire rings. Figure 2.16 shows the components of a typical clutch cover assembly.

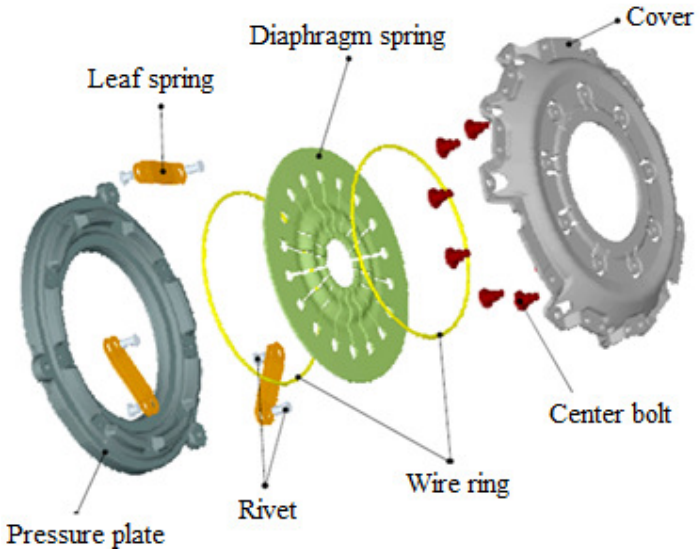

Figure 2.16 : Components of the clutch cover assembly [21].

The clutch cover transmits the engine torque to the clutch disc via the housing, the tangential leaf springs and the pressure plate during the clutch engagement. The pressure plate is assembled to the clutch cover via tangential leaf springs. Tangential leaf springs account for transferring the engine torque to the pressure plate from the clutch cover, moving the pressure plate during clutch disengagement as well as center aligning.

The pressure plate transfers the axial force, which is also called clamp load. It pushes the clutch plate to the flywheel, so that the clutch disc gets interposed between the pressure plate and the flywheel. The pressure plate and the cover are kept together by leaf springs. While the clutch is engaged, these springs deflect and thereafter transfer the torque from the cover to the pressure plate without any friction between them [21]. The second function of the leaf springs is that during clutch disengaging process, the leaf springs pulls the pressure plate away from the clutch disc assembly [23].

The pressure plate might be exposed to high slippage during abusive clutch engagement, and kinetic energy can generate heat, eventually causing high peak temperatures. At high temperatures, even distortions may occur. Hence, adequate rigidity is required. Another reason why rigidity is needed is that the pressure plate must provide as uniform a pressure as possible. Also, the component should have sufficient mass and high thermal conductivity to cool itself down. Due to all of these reasons, high tensile grey iron is the most optimal and commonly used material for the pressure plate [21].

Diaphragm springs are pretensioned belleville springs with integrated actuating levers. They axially press the pressure plate to the clutch disc and lift it when the clutch is engaged and disengaged, respectively. Wire rings are located in the clutch cover to support the diaphragm spring. When the spring fingers move to the engine side, the edge of the inner wire ring bends away from the engine and takes the pressure plate back to the transmission side.

The shape and the material of the diaphragm spring are substantial in terms of operating comfort and service life. The typical material is high quality spring steel. The diaphragm spring characteristic is designed such that the clamp load increases for the first phase of the clutch wear and reaches to a maximum value. Then it

decreases to its original new value while the facing wear is at maximum. Due to this characteristic, the clutch continues to operate without any trouble [14,24]. The typical clamp load curve for a diaphragm spring is given in Figure 2.17.

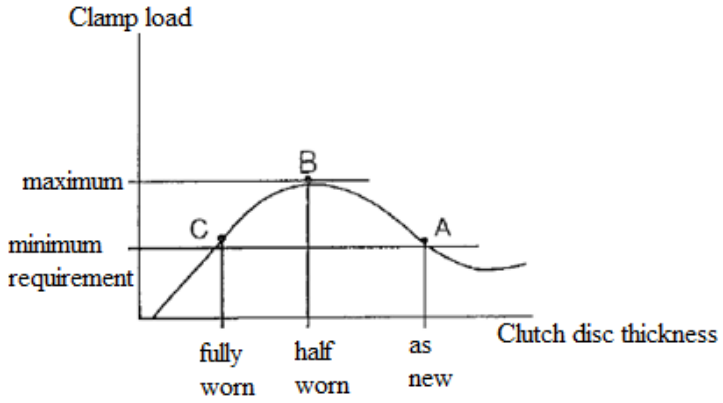

Figure 2.17 : Typical clamp load curve of the diaphragm springs [24].

Figure 2.18 indicates the several clutch characteristic curves. The y-axis on the left and on the right specify the load and the pressure plate lift, respectively as the x-axis represents the release travel. The dotted line shows the release load characteristic curve, which is the load on the release bearing to actuate the clutch. The release load rises as the clutch linings are worn out.

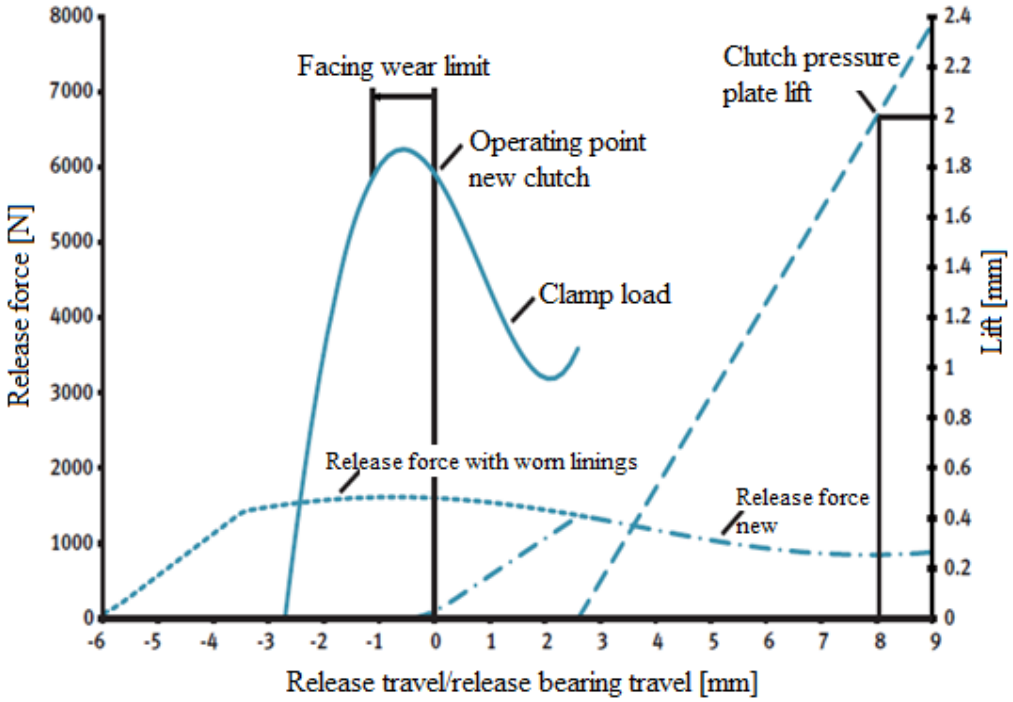

Figure 2.18 : Clutch characteristic curves [9].

The dashed line in Figure 2.18 is the pressure plate displacement with respect to the release bearing travel. From the lift off curve, clutch lever ratio is determined, which is ratio of the release travel to the lift off.

2.5.3 Clutch release bearing

The clutch release bearing is used to transmit the force that is delivered from the clutch actuation system to the diaphragm spring in order to disengage the clutch. It is mounted to the diaphragm spring with a snap-ring and a coupler. It rotates at the engine speed and slides on a guiding tube of the transmission [26]. The appearance of a clutch release bearing is shown in Figure 2.19.

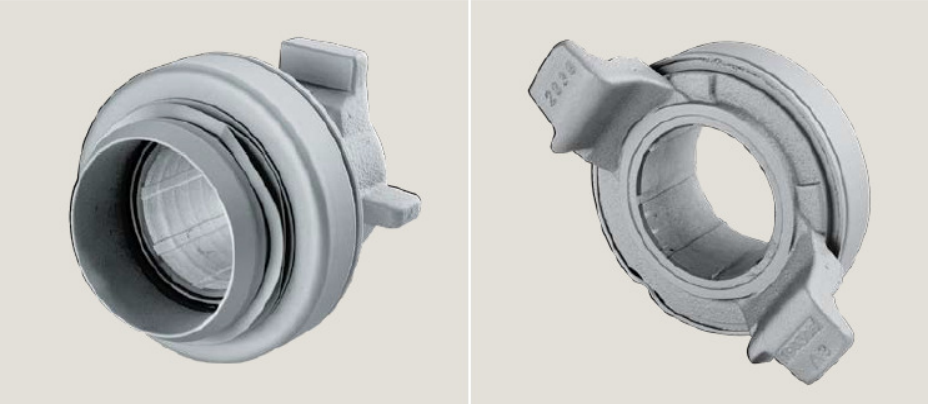

Figure 2.19 : Clutch release bearing assembly [24].

Depending on the clutch type, the place where the release bearing is retained varies. In a push-type clutch system, the releaser rests on the tips of the diaphragm spring, whereas in a pull-type clutch system it is locked accordingly for the safety of the assembly. This makes the pull-type clutch more complex than a push-type clutch, as it is subjected to high axial forces. Hence, the release bearing must absorb high axial forces in this respect [14].

2.5.4 Flywheel

The flywheel is bolted to the crankshaft and rotates with the engine speed. It is a large metallic disc in appearance and made of cast iron in most cases. It provides a friction surface for the clutch disc and sandwiches it with clutch cover. Figure 2.20 shows a typical engine flywheel utilized in heavy duty vehicles.

Figure 2.20 : Flywheel assembly [25].

The main functions of the flywheel are:

a) To reduce acyclism with inertia: Due to the explosions in engine cylinders, acyclism occurs at crankshaft since the torque generation is not constant. Flywheel inertia helps smooth the variations in engine torque together with the crankshaft and clutch cover.
b) To maintain the clutch cover assembly.
c) To provide friction surface for the clutch disc.
d) To dissipate energy due to friction.
e) To store and release energy from the crankshaft [25].

The Ford Trucks are equipped with a rigid solid mass flywheel.

2.5.5 Clutch release system

The basic purpose of the clutch release system is to convert the mechanical force generated by the clutch pedal into a force acting on the clutch lever throughout a hydraulic linkage.

The clutch release system consists of a hydraulic subsystem. It is comprised of the clutch master cylinder with a hydraulic reservoir mounted to the clutch pedal, the

clutch servo mounted to the clutch housing and a hydraulic pressure line between the two, which is illustrated in Figure 2.21.

The clutch release loads of the trucks with high engine torques are high, which may result in unacceptably heavy pedal loads. To overcome this problem, the clutch servo with air support in addition to hydraulic system are utilized. The air is supplied to the clutch servo as proportional to pedal loads.

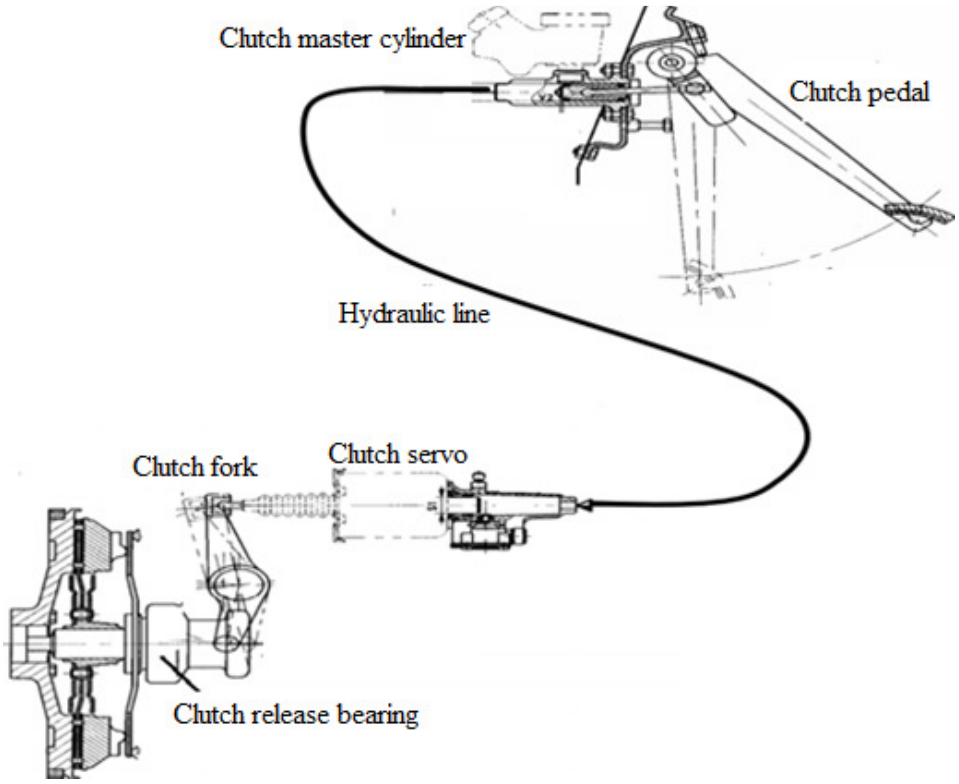

Figure 2.21 : Typical clutch actuation system of a heavy duty clutch [26].

When the driver depresses the clutch pedal, the pedal stroke is transferred to the clutch master cylinder so far as the clutch pedal ratio. The piston inside the clutch master cylinder moves toward the hydraulic line due to the mechanical force generated by the driver's foot. In return, hydraulic line is pressurized. The pressurised hydraulic line pushes the hydraulic piston and the push rod connected to it inside the clutch servo. The push rod pushes the clutch release fork, and finally disengages the clutch. There is no torque transfer as the clutch pedal is depressed.

There are numerous parameters considered in clutch release system design. Mainly, they are:

a) System's life expectancy, namely, the number of release cycles specified during service life.
b) The ratios of the clutch master cylinder and the clutch servo in order to meet the required pedal forces and release strokes.
c) Operating conditions, which include the specified operating pressure and temperature range, clearances to other components [22].

3. THEORY

3.1 Clutch Torque Capacity

Torque transmissibility of the clutch is one of the key factors in clutch design. The transmittable torque through the clutch is a function of its geometry, the actuating force of the clutch cover and the properties of the friction material.

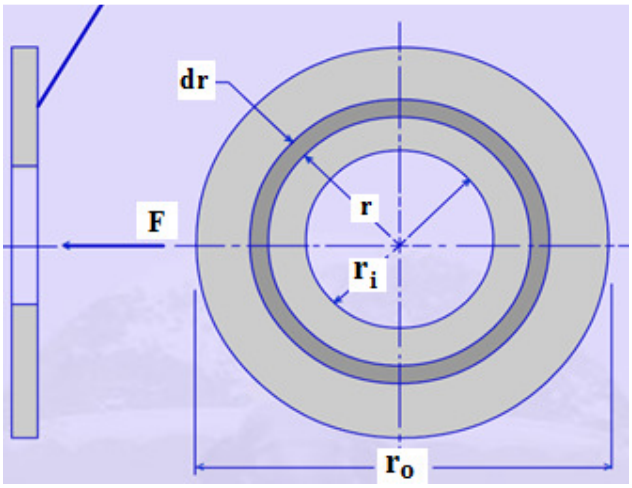

Figure 3.1 : Single surface axial disc clutch [27].

Assuming an uniform pressure from the geometry in Figure 3.1, the elemental area can be obtained in **(3.1).**

$$dA = 2\pi r dr \tag{3.1}$$

(3.2) states the normal force exerted on this elemental area:

$$dN = 2\pi p r dr \tag{3.2}$$

where p is the total pressure on the clutch linings generated by the clutch cover.

In return, the frictional force dF on this area can be seen in **(3.3).**

$$dF = 2\pi p \mu r dr \tag{3.3}$$

where μ is the coefficient of the friction between the sliding surfaces.

The torque transmitted through the elemental area depends on the frictional force and the moment arm around the radius r. The equation is given in **(3.4)** and it can also be written in the form of **(3.5)** and **(3.6)**.

$$dT = dFr = \mu dNr = \mu pAr \quad \textbf{(3.4)}$$

$$dT = 2\pi r\mu prdr \quad \textbf{(3.5)}$$

$$dT = 2\pi\mu pr^2 dr \quad \textbf{(3.6)}$$

Integrating **(3.6)** between the inner and outer radius of the clutch yields the total torque that can be transmitted through the clutch, as shown in **(3.7),** and **(3.8)** after the integration.

$$T = \int_{r_i}^{r_o} 2\pi\mu pr^2 dr \quad \textbf{(3.7)}$$

$$T = \frac{2}{3}\pi\mu p({r_o}^3 - {r_i}^3) \quad \textbf{(3.8)}$$

The actuation force which is required to apply for the total torque transmitted through the clutch is obtained by the inegration of the normal force between the inner and the outer diameter of the clutch, as given in (**3.9**).

$$F_a = \int_{r_i}^{r_o} 2\pi prdr \quad \textbf{(3.9)}$$

$$F_a = \pi p({r_o}^2 - {r_i}^2) \quad \textbf{(3.10)}$$

Combining **(3.8)** and **(3.10)** gives the torque equation as seen in **(3.11).**

$$T = \frac{2}{3}\frac{({r_o}^3 - {r_i}^3)}{({r_o}^2 - {r_i}^2)}\mu F_a \quad \textbf{(3.11)}$$

where $\frac{2}{3}\frac{({r_o}^3 - {r_i}^3)}{({r_o}^2 - {r_i}^2)}$ is the mean radius of the clutch and denoted by R_m. **(3.11)** finally becomes:

$$T = R_m\mu F_a \quad \textbf{(3.12)}$$

(3.12) gives the torque equation for a single surface. Denoting the number of the frictional discs in contact as N, the torque equation finally becomes;

$$T = NR_m\mu F_a \quad \textbf{(3.13)}$$

$$N = n_1 + n_2 - 1 \quad \textbf{(3.14)}$$

where n_1 and n_2 in **(3.14)** are the number of the driving and the driven discs, respectively.

Equation **(3.13)** is the final result of the clutch torque capacity and relates the amount of transmittable engine torque through the clutch, based on its properties.

3.2 Clutch Torque During Vehicle Launch

The configuration of a rear wheel driven vehicle with a manual transmission is illustrated in Figure 3.2. The powertrain consists of an engine, a clutch, a transmission, a propeller shaft, a differential and driveshafts connected to the wheels.

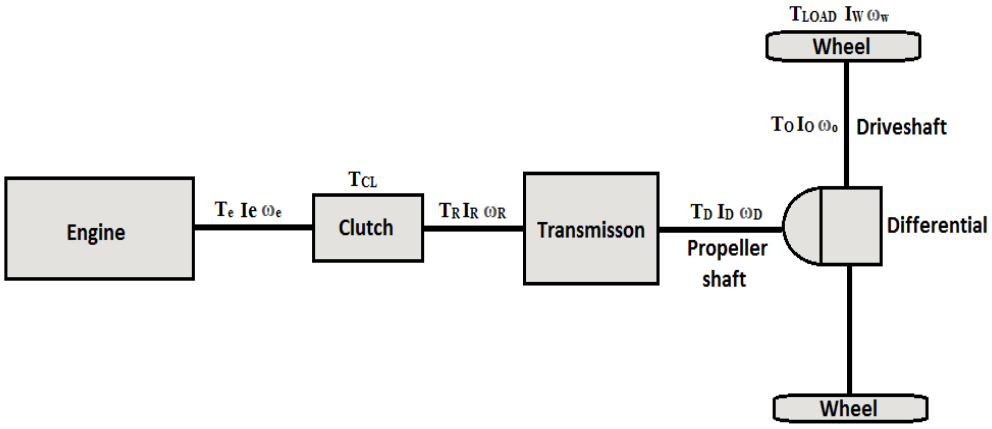

Figure 3.2 : Illustration of the powertrain for a rear wheel driven vehicle.

In the following equations, the engine output torque, clutch torque, transmission output torque, propeller shaft output torque and driveshaft output torque are denoted by T_e, T_{CL}, T_R, T_D and T_O, respectively. In a similar fashion, I_e, I_R, I_D, I_O and $\omega_e, \omega_R, \omega_D, \omega_O$ denote the respective mass moment of inertias and angular velocities of the engine, the transmission, the propeller shaft and the driveshaft. T_{LOAD}, I_W and ω_W represent the road load torque, equivalent mass moment of inertia of the vehicle on driveshaft, and the angular velocity of the wheels, respectively.

The equations of the motion of the system are given as **(3.15), (3.16), (3.17), (3.18), (3.19)** [28]:

$$T_e - T_{CL} = I_e \acute{\omega}_e \qquad \textbf{(3.15)}$$

$$T_{CL} - T_R = I_R \acute{\omega}_R \qquad \textbf{(3.16)}$$

$$T_R - \frac{T_D}{I_1} = I_D \acute{\omega}_D \quad \textbf{(3.17)}$$

$$T_D - \frac{T_O}{I_{FD}} = I_O \acute{\omega}_O \quad \textbf{(3.18)}$$

$$T_O - T_{LOAD} = I_W \acute{\omega}_W \quad \textbf{(3.19)}$$

where I_1 is the first gear ratio and I_{FD} is the final drive ratio.

and $\acute{\omega}_e$, $\acute{\omega}_R$, $\acute{\omega}_D$, $\acute{\omega}_O$ and $\acute{\omega}_W$ represent the respective angular accelerations of the engine, the transmission, the propeller shaft, the driveshaft and the wheels.

The road load torque is the sum of the resistance torques and can be expressed as in **(3.20)** [28].

$$T_{LOAD} = (fW + R_A + R_G)r \quad \textbf{(3.20)}$$

where f is the rolling resistance coefficient, W is vehicle mass, r is tire radius, R_A is the air resistance force and R_G is the grade resistance force.

The air resistance force is expressed in **(3.21)**.

$$R_A = \frac{C_D A_F \rho V^2}{2} \quad \textbf{(3.21)}$$

where C_D, A_F, ρ, V are the air drag coefficient, the frontal cross section area of the vehicle, the air density and the vehicle speed, respectively.

The grade resistance force is given in **(3.22)**.

$$R_G = Wg \sin \alpha \quad \textbf{(3.22)}$$

where g and α are the gravitational acceleration and the slope of the road in degree, respectively.

The angular velocities can be presented in **(3.23)**, as well as **(3.24), (3.25)** depending on the gear ratios.

$$\omega_w = \omega_o \quad \textbf{(3.23)}$$

$$\omega_D = \omega_W I_{FD} \quad \textbf{(3.24)}$$

$$\omega_R = \omega_W I_{FD} I_1 \quad \textbf{(3.25)}$$

From **(3.16), (3.17), (3.18)** and **(3.19),** clutch torque T_{CL} can be expressed in terms of only the wheel acceleration since it is easier to measure the data from the wheels than measuring from the shafts, finally giving the clutch torque equation **(3.26)**,

$$T_{CL} = \acute{\omega}_W \left(\frac{I_W}{I_{FD} I_1} + \frac{I_O}{I_1} + I_D I_{FD} + I_R I_{FD} I_1 \right) + \frac{T_{LOAD}}{I_{FD} I_1} \quad \textbf{(3.26)}$$

According to Equation **(3.26),** during the vehicle launch, the clutch torque increases until it is fully engaged.

3.3 Heat Energy Generation During Clutch Engagement

During the clutch engagement, the kinetic energy due to the velocity differences between the driving and the driven shafts is converted to heat energy.

First, integrating **(3.15)** and **(3.16)** for the initial conditions between the time frame 0 to t gives **(3.27)** and **(3.28),** and at t=0, $\omega_e = \Omega_e$ and $\omega_R = \Omega_R$

$$\omega_e = \frac{T_e}{I_e} t - \frac{1}{I_e} \int_0^t T_{CL} dt + \Omega_e \quad \textbf{(3.27)}$$

$$\omega_R = -\frac{T_R}{I_R} t - \frac{1}{I_R} \int_0^t T_{CL} dt + \Omega_R \quad \textbf{(3.28)}$$

$$\omega_{ra} = \omega_e - \omega_R \quad \textbf{(3.29)}$$

where ω_{ra} in **(3.29)** states the relative angular velocity,

Substracting **(3.28)** from **(3.27)** yields **(3.30)**:

$$\omega_{ra} = Kt - L \int_0^t T_{CL} dt + \omega_{ro} \quad \textbf{(3.30)}$$

where

$$K = \frac{T_e}{I_e} + \frac{T_R}{I_R} \quad \textbf{(3.31)}$$

$$L = \frac{1}{I_e} + \frac{1}{I_R} \quad \textbf{(3.32)}$$

$$\omega_{ro} = \Omega_e - \Omega_R \quad \textbf{(3.33)}$$

Considering that there is no external torque, **(3.30)** becomes:

$$\omega_{ra} = -L \int_0^t T_{CL} dt + \omega_{ro} \quad \textbf{(3.34)}$$

The slipping period is determined in **(3.35),** by putting $\omega_{ra} = 0$ in **(3.34)**.

$$\omega_{ro} = L\int_0^t T_{CL}\,dt \quad \textbf{(3.35)}$$

There are three different cases where the slipping time varies with respect to the applied pressure (or torque). In any of these situations, the clutch torque changes as well.

a) Constant pressure
b) Linearly increasing pressure
c) Parabolically increasing pressure

3.3.1 Constant pressure

The pressure for this case is [29].

$$P_{max(t)} = P_{max(0)}$$

(3.36) states the clutch torque, considering constant pressure;

$$T_{CL} = P_{max(t)}\mu\pi r_i(r_o{}^2 - r_i{}^2) = T_1 \quad \textbf{(3.36)}$$

Slipping period t_s in **(3.37)** is obtained by equating ω_{ro} to 0 in **(3.35),**

$$t_s = \frac{\omega_{ro}}{LT_1} \quad \textbf{(3.37)}$$

The relative angular velocity $\omega_{r(t)}$ can be obtained from **(3.34)**

$$\omega_{r(t)} = \omega_{ro}\,(1 - \frac{1}{t_s}) \quad \textbf{(3.38)}$$

The total heat energy dissipated on the clutch during a single engagement for the constant pressure situation is expressed in **(3.39)**

$$Q_{H,C} = \frac{1}{2} f_c r_i A\mu P_{max(0)}\omega_{ro} t_s \quad \textbf{(3.39)}$$

$$A = n\pi(r_o{}^2 - r_i{}^2) \quad \textbf{(3.40)}$$

In **(3.40)**, A is the total contact surface area, n is the number of contact surfaces and f_c is the heat partition ratio. The heat partition ratio determines the proportion of the heat that enters to the sliding components of the clutch, namely, flywheel, clutch disc and pressure plate.

In most cases, the flywheel and pressure plate are made of the same material. The equation of the heat partition ratio is given in **(3.41)** [30].

$$f_c = \frac{\sqrt{k_d \rho_d c_d}}{\sqrt{k_d \rho_d c_d} + \sqrt{k_f \rho_f c_f}} \quad \textbf{(3.41)}$$

where k is the thermal conductivity, ρ is the density and c is the specific heat. The subscript d and f refer to the clutch disc and flywheel, respectively.

3.3.2 Linearly increasing pressure

The pressure function in this case is [29].

$$P_{max(t)} = P_{max(0)}\left(\frac{t}{t_s}\right)$$

(3.42) states the clutch torque, considering linearly increasing pressure;

$$T_{CL} = T_1\left(\frac{t}{t_s}\right) = P_{max(0)}\left(\frac{t}{t_s}\right)\mu\pi r_i\left(r_o{}^2 - r_i{}^2\right) \quad \textbf{(3.42)}$$

The slipping period in **(3.43)** and relative angular velocity **(3.44)** can be obtained by following the same procedures applied for the constant pressure case

$$t_s = \frac{2\omega_{ro}}{LT_1} \quad \textbf{(3.43)}$$

$$\omega_{r(t)} = \omega_{ro}\left(1 - \left(\frac{1}{t_s}\right)^2\right) \quad \textbf{(3.44)}$$

The total heat energy dissipated on the clutch during a single engagement for the linearly increasing pressure situation is expressed in **(3.45)**.

$$Q_{H,L} = \frac{1}{4} f_c r_i A \mu P_{max(0)} \omega_{ro} t_s \quad \textbf{(3.45)}$$

3.3.3 Parabolically increasing pressure

The pressure function for parabolically increasing pressure is [29].

$$P_{max(t)} = P_{max(0)}\left(\frac{t}{t_s}\right)\left(2 - \frac{t}{t_s}\right)$$

(3.46) states the clutch torque, followed by **(3.47)** and **(3.48),** considering parabolically increasing pressure;

$$T_{CL} = T_1\left(\frac{t}{t_s}\right)\left(2 - \frac{t}{t_s}\right) \quad \textbf{(3.46)}$$

$$T_{CL} = P_{max(0)}\left(\frac{t}{t_s}\right)\mu\pi\left(2 - \frac{t}{t_s}\right) r_i\left(r_o{}^2 - r_i{}^2\right) \quad \textbf{(3.47)}$$

$$T_{CL} = T_1 \left(\frac{t}{t_s}\right)\left(2 - \frac{t}{t_s}\right) \quad \textbf{(3.48)}$$

Then, the slipping time can be found in **(3.49)**

$$t_s = \frac{3\omega_{ro}}{2LT_1} \quad \textbf{(3.49)}$$

The relative angular velocity can be found in **(3.50)**

$$\omega_{r(t)} = \omega_{ro}\left(\frac{1}{2}\left(\frac{1}{t_s}\right)^3 - \frac{1}{3}\left(\frac{1}{t_s}\right)^2 + 1\right) \quad \textbf{(3.50)}$$

The total heat energy dissipated on the clutch during a single engagement for the parabolically increasing pressure situation is expressed in **(3.51)**.

$$Q_{H,P} = \frac{1}{3} f_c r_i A \mu P_{max(0)} \omega_{ro} t_s \quad \textbf{(3.51)}$$

3.4 Heat Dissipation During Clutch Engagement

The heat generated in the clutch will dissipate through the frictional components and to the environment. The sliding components will heat up due to friction as the convective heat transfer takes place to environment [31].

The temperatures of the sliding components will change at each step, and the heat equation is given in **(3.52)** [32].

$$Q_H - Q_{conv} = m\, C_p \frac{dT}{dt} \quad \textbf{(3.52)}$$

In **(3.52)**, Q_{conv} is the convective heat lost from the clutch to the air within the clutch housing. The rest of the thermal energy will change the temperature of the clutch components. Knowing the heat partition ratios, the temperature increments of the components per each period individually can be obtained from **(3.52)**.

The equation for the temperature of the air within the clutch housing is given in **(3.53)**:

$$Q_{conv} - Q_{out} = m_a C_{p,a} \frac{dT_a}{dt} \quad \textbf{(3.53)}$$

where Q_{out} is the heat convected to the clutch housing case.

In **(3.53)**, the subscript a refers to the air in the clutch housing.

Q_{out} can be mentioned in **(3.54)**:

$$Q_{out} = h_a A_a (T_a - T_c) \quad \textbf{(3.54)}$$

where h_a and A_a are heat transfer coefficient and area of convection, respectively.

The heat equation for the temperature of the clutch housing case is expressed in (**3.55**) [34].

$$Q_{c,in} - Q_{c,out} = m_c C_{p,c} \frac{dT_c}{dt} \quad \textbf{(3.55)}$$

where $Q_{c,in}$ and $Q_{c,out}$ are the amount of heat convected from the air inside the housing and the amount of heat conducted to ambient air outside of the housing, respectively. The subscript c indicates the clutch housing case.

The amount of heat convected to ambient air can be expressed as in **(3.56)** [34].

$$Q_{c,out} = k_c A_c (T_c - T_{amb}) \quad \textbf{(3.56)}$$

where k, A and T_{amb} are the conductivity of air, area of the convection of the clutch housing and ambient temperature outside of the clutch housing, respectively.

4. TESTING

4.1 Vehicle Configurations

Three different types of trucks were undergone the clutch hill start test. Each truck has different engine output torque and power as well as purpose of usage. The selection of the trucks was made such that the traction force at wheels was minimum so that the slippage in the clutch was maximum. The properties of the vehicles are given in Table 4.1.

Table 4.1 : Vehicle properties.

Vehicle ID	Vehicle 1	Vehicle 2	Vehicle 3
Vehicle type	Road Truck	Mixer	Tractor
Clutch Type	Single disc - dry	Single disc - dry	Single disc - dry
Series	3232C	4142M	1846T
Engine displacement – [L]	9	11.3	12.7
Number of engine cylinders	6	6	6
Drive	8x2	8x4	4x2
Wheelbase - [mm]	5500	5100	3600
Maximum engine torque - [Nm]	1300	2000	2300
Maximum engine power - [PS]	330	420	460
Maximum vehicle mass - [kg]	35500	41000	43000
Transmission ratio	9.48	13.8	13.8
Final drive ratio	4.63	3.76	2.85
Tire type	315/80R22.5	315/80R22.5	12R/22.5
Clutch effective mean radius - [mm]	172	172	172

Vehicle 1 is a road truck and it is 3233C series, where 32, 33 and C imply the gross total mass (GTM) in tons, one-tenth of the maximum engine power in PS, and the command steer respectively. The vehicle is utilized for on-road purposes and carries the payload via its trailer mounted on the chassis. The Vehicle 1 is illustrated in Figure 4.1.

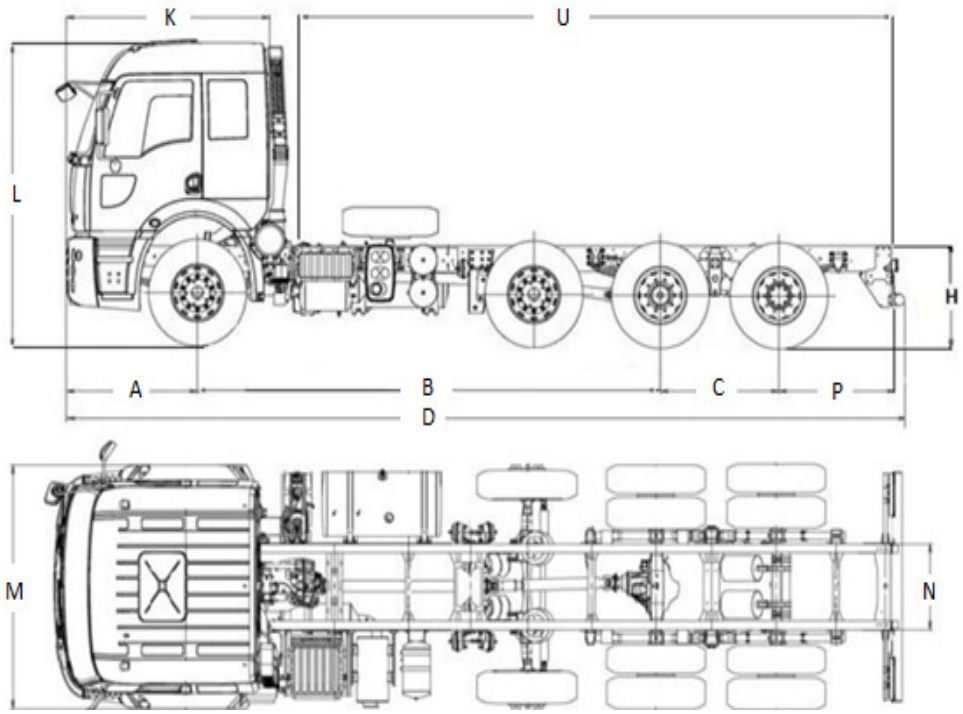

Figure 4.1 : Dimensions of the Vehicle 1 [29].

The relevant dimensions of the vehicle from Figure 4.1 are tabulated in Table 4.2.

Table 4.2 : Dimensions of the Vehicle 1 [29].

Vehicle dimensions		
Sign	Description	Dimension [mm]
A	Front length	1465
B	Wheelbase	5500
C	Distance between rear axles	1305
D	Maximum length	9350
H	Chassis height	1125
K	Cabin length	2225
L	Maximum height	3910
M	Width	2489
N	Chassis width	866
P	Rear length	935
U	Useful chassis length	6705

A photo of the Vehicle 1 during the preparation for the test is shown in Figure 4.2.

Figure 4.2 : Vehicle 1 during the test preparation.

Vehicle 2 is a mixer truck and it is 4142M series. The vehicle is utilized for off-road purposes and carries construction goods such as cement via its superstructure mixer mounted through the chassis. Also, it is equipped with an engine power take off unit to be able to rotate the shaft connected to mixer to keep the material in a liquid state. The engine power take off unit uses up additional torque from the engine since it is a seperated driven shaft. Due to its nature, the vehicle is subjected to more frequent clutch engagement and disengagement than road trucks. The vehicle is illustrated in Figure 4.3.

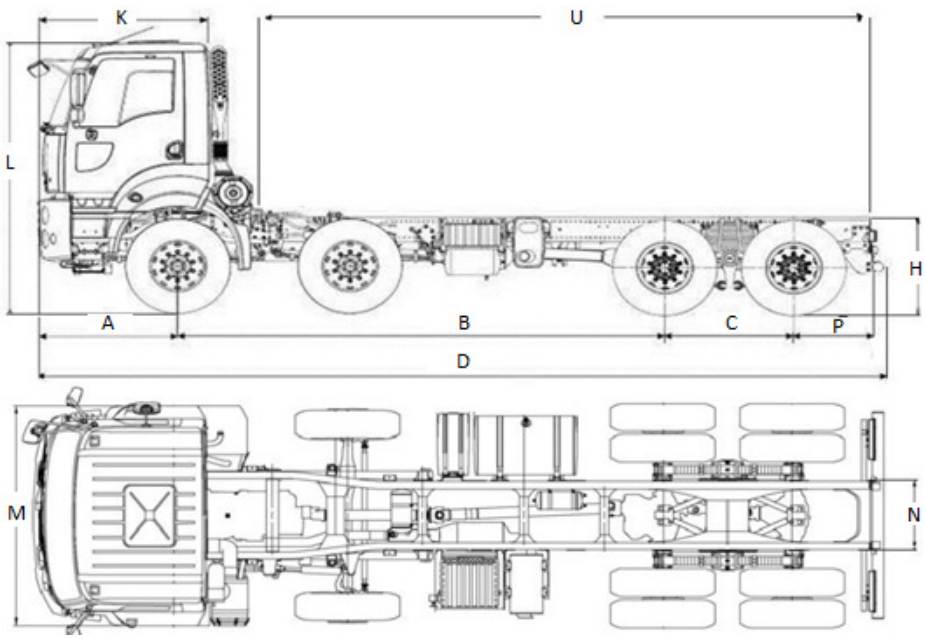

Figure 4.3 : Dimensions of the Vehicle 2 [30].

The relevant dimensions of the vehicle from Figure 4.3 are tabulated in Table 4.3.

Table 4.3 : Dimensions of the Vehicle 2 [30].

Vehicle dimensions		
Sign	Description	Dimension [mm]
A	Front length	1461
B	Wheelbase	5100
C	Distance between rear axles	1350
D	Maximum length	8886
H	Chassis height	1160
K	Cabin length	1745
L	Maximum height	3220
M	Width	2250
N	Chassis width	986
P	Rear length	800
U	Useful chassis length	6691

A photo of the Vehicle 2 during warm-up prior to the test is shown in Figure 4.4.

Figure 4.4 : Vehicle 2 during warm-up.

Vehicle 3 is yet another road truck, which is called tractor and it is 1846T series, where 18, 46 and T imply gross vehicle mass (GVM) in tons, which means the maximum allowable mass carried without trailer, one-tenth of maximum engine power in PS, and tractor respectively. The vehicle is utilized for on-road purposes and carries the payload via its trailer mounted on the chassis. The prominent differences between the Vehicle 1 and the Vehicle 3 are that the Vehicle 3 has a

shorter wheelbase and different trailer connection points onto the chassis. The vehicle is illustrated in Figure 4.5.

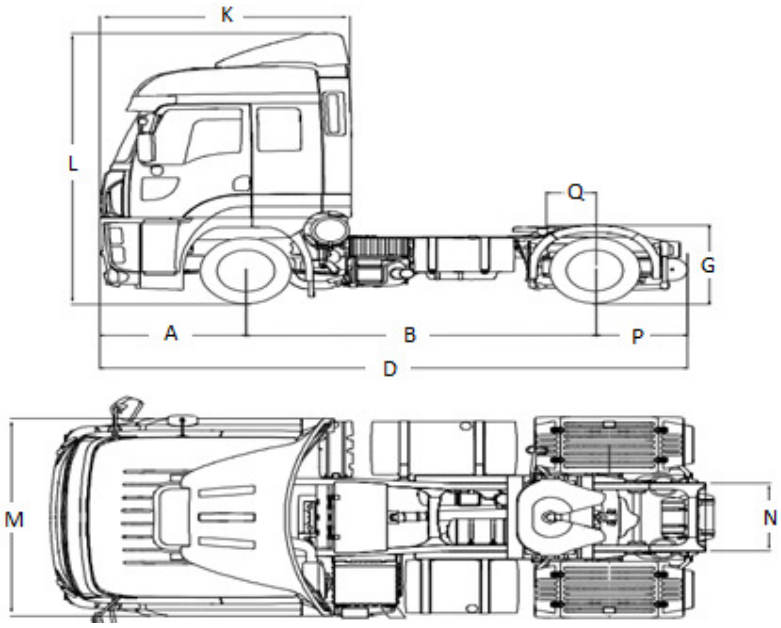

Figure 4.5 : Dimensions of the Vehicle 3 [31].

The relevant dimensions of the Vehicle 3 from Figure 4.5 are tabulated in Table 4.4.

Table 4.4 : Dimensions of the Vehicle 3 [31].

Vehicle dimensions		
Sign	Description	Dimension [mm]
A	Front length	1500
B	Wheelbase	3600
D	Maximum length	6044
G	Fifth tire height (laden)	966
K	Cabin length	2581
L	Maximum height	3678
M	Width	2489
N	Chassis width	866
P	Rear length	954
Q	Fifth tire location	590

The Vehicle 3 during the test can be seen in Figure 4.6.

Figure 4.6 : Vehicle 3 during the test.

4.2 Clutch Hill Start Test

The test is performed to determine thermal effects in the clutch when the it is subjected to a number of starts at short regular intervals with a fully loadad vehicle on a slope. The thermocouples measure the temperature of the air within the clutch housing. The components and final temperatures are examined after the test.

4.2.1 Instrumentation

Prior to the test, thermocouples are placed at appropriate places in the clutch housing such as near the clutch release bearing from the inspection hole and the flywheel by drilling the clutch housing.

Continuous temperature measurement from the sensors is crucial for interpreting the test. Therefore, it is important to check all instrumentions work properly and arrange wires and routings for the sensors.

A cross section view of the clutch system for the vehicles is shown in Figure 4.7. As seen from the figure, there is a little space inside the clutch housing, which means the thermocouple locations are quite limited for most of the cases.

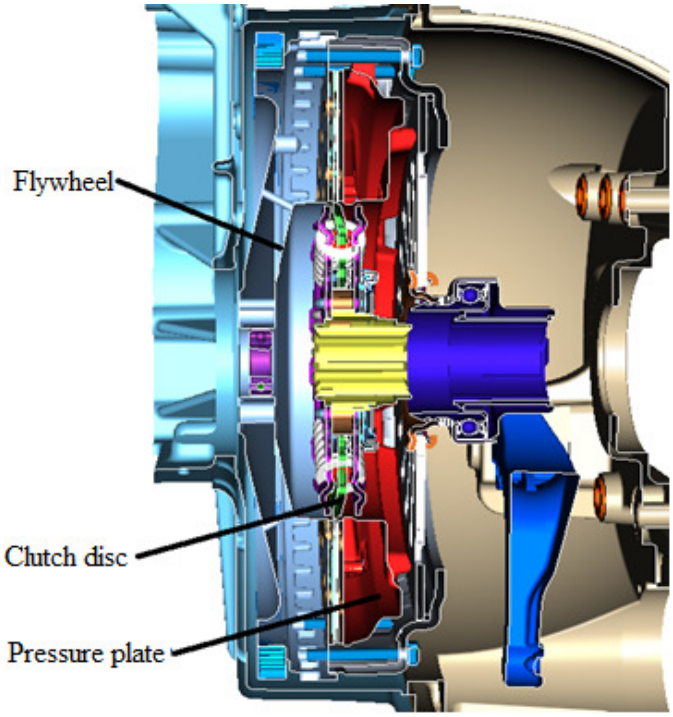

Figure 4.7 : Cross section view of the clutch system

Figure 4.8 shows the thermocouple placed right near the clutch release bearing.

Figure 4.8 : Thermocouple position near clutch release bearing.

Another thermocouple is put near the flywheel by piercing the surface of the clutch housing, which is shown in Figure 4.9.

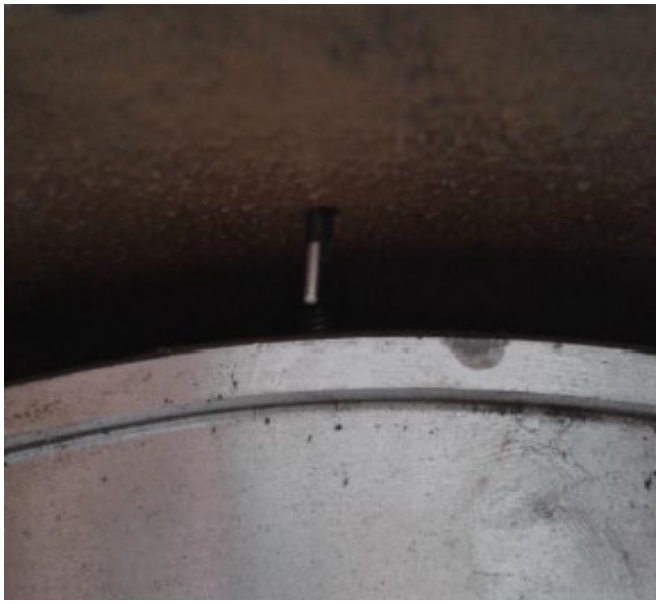

Figure 4.9 : Thermocouple position near flywheel.

4.2.2 Test preparation and procedure

The test is performed according to the following procedure:

a) Part replacements are completed and test equipments are prepared. Thermocouples are installed near clutch release bearing and engine flywheel to measure air temperature in clutch housing. All the thermocouples and wiring routings are checked to make sure they work properly.

b) After all instrumentations are done, clutch bedding is performed with the fully loaded vehicle. The vehicle is driven at a moderate speed without any kind of irregular behavior such as abrupt clutch engagement or disengagement.

c) The test begins on a road with 10% slope once the air temperature within the clutch housing reaches to 80 °C.

d) Hand brake is applied and the lowest gear is selected.

e) Clutch pedal and handbrake are released while the accelerator pedal is operated. The vehicle is driven in a normal manner at a minimum determined drive speed such that the engine speed is still sufficiently high to continue to drive up the hill.

f) The air within the clutch housing temperature is recorded after each start, until the test is completed.

g) The aforementioned steps are repeated at 1 minute intervals for 100 cycles.

4.2.3 Test facility

Tests were conducted in Valeo Turkey's Bursa City facilities, as seen in Figure 4.11.

Figure 4.10 : Test facility in Bursa.

Test and test facility information are shown in Table 4.5.

Table 4.5 : Test facility and dates.

Vehicle	Vehicle 1	Vehicle 2	Vehicle 3
Road slope – [%]	10		
Road type	Asphalt		
Ambient temperature – [°C]	10	10	21
Test date – [dd.mm.yyyy]	01.11.2013	28.02.2014	19.03.2014

As used here, the ambient temperature refers to the weather temperature.

5. SIMULATION AND RESULTS

5.1 Model

The model consists of mainly five sections. Sections are linked to each other accordingly in the model as shown in Figure 5.1.

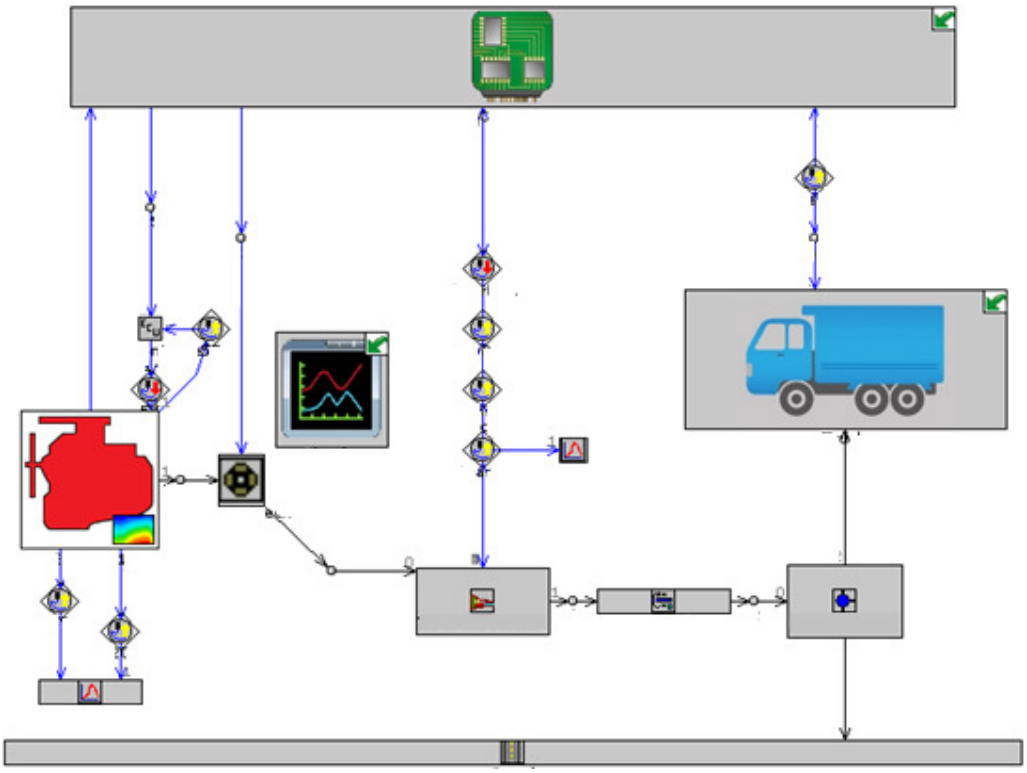

Figure 5.1 : Basic model on GT-SUITE.

5.1.1 Control section

In the control section, the steps in the test procedure are modeled. Gearshifting and braking strategy as well as clutch and gas pedal modulations are created. The virtual driver releases the clutch pedal, depresses the gas pedal, shifts the gear and drives the vehicle at a target speed as a function of the engine speed, gear ratios and tire size. Then the vehicle waits at the idle speed for 1 minute and repeats the same cylcle for 100 times until the simulation is finished. These are achieved by the controller

module and other connections in the control section linked to each other accordingly, seen in Figure 5.2.

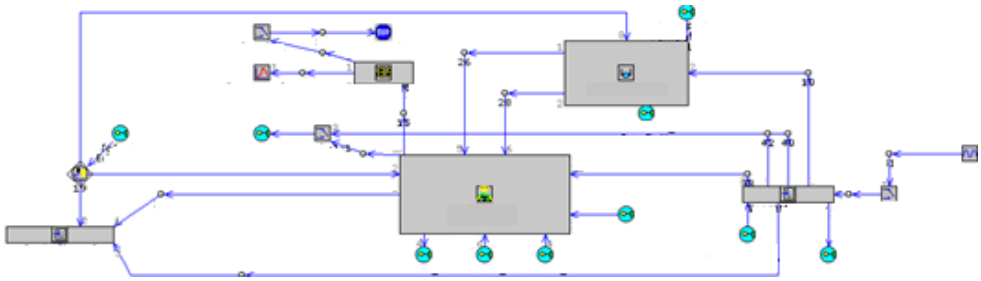

Figure 5.2 : Control section of the model.

5.1.2 Clutch mechanical section

Figure 5.3 shows the clutch module that is placed between the crankshaft and transmission input shaft, both of which rotate at different angular speeds until the synchronization is established. The moment of inertias of both shafts are also inserted. The mean radius of the clutch, the clamp load of the clutch cover and the variation graph of the clutch friction coefficient with respect to temperature are placed in the clutch module. The information from the clutch mechanical section is sent to the clutch thermal section at every step of the simulation.

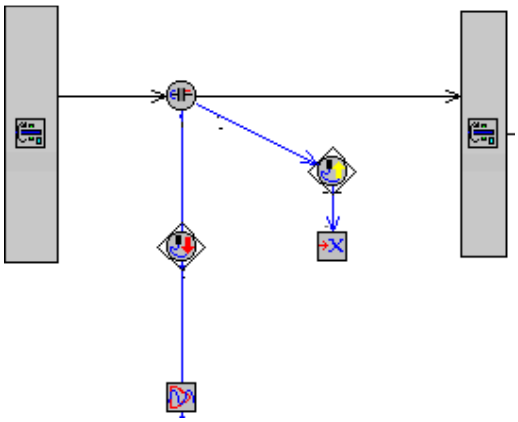

Figure 5.3 : Clutch mechanical section of the model.

5.1.3 Clutch thermal section

According to the Figure 5.4, the frictional clutch mass is connected to the clutch housing by means of the air inside the clutch housing, while it is connected to the ambient air outside of the clutch housing. Mass and material information of the clutch and clutch housing, the conduction and the convection heat transfer

coefficients of the clutch and the air inside the clutch housing are put into clutch thermal section. The heat generated in the clutch heats the clutch itself first, then the energy goes to the clutch housing by air. The heat is then convected from the clutch housing to the ambient air outside of the housing. The clutch housing mass and surface area are correlated for the heavy commercial vehicles based on a former test performed in the past.

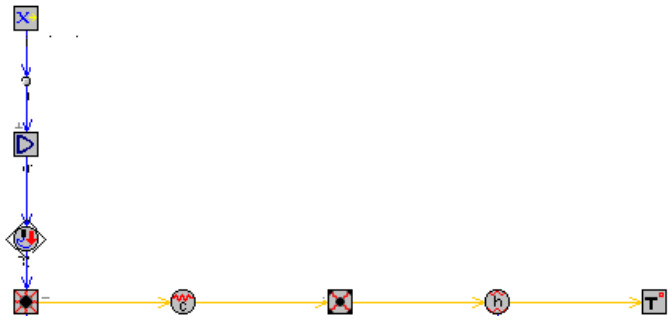

Figure 5.4 : Clutch thermal section of the model.

5.1.4 Vehicle section

The vehicle section consists of the main vehicle body and powertrain components such as transmission, driveshaft, differential, axles and tires. These elements are linked on each other with rigid connections as shown in Figure 5.5. Ultimately, the vehicle is connected to the road by tires and to the control section accordingly.

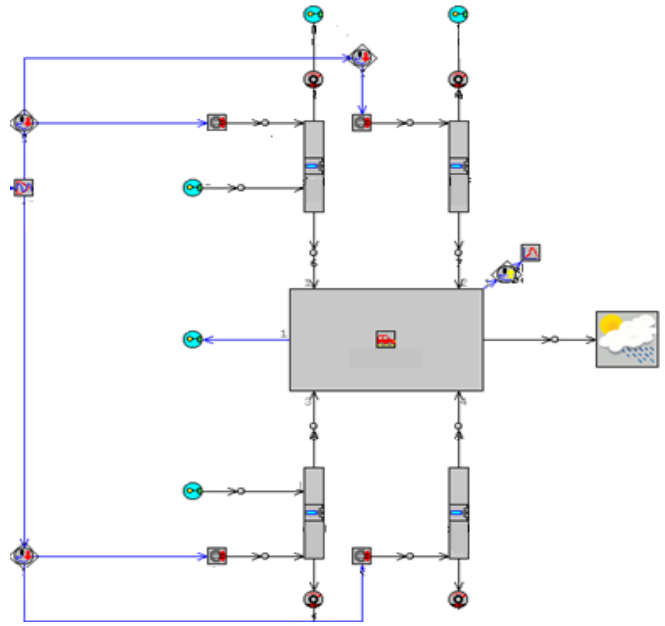

Figure 5.5 : Vehicle section of the model.

5.1.5 Engine section

The torque map is inserted to the engine section so that the clutch benefits the torque as a function of the engine speed, clutch and gas pedal adjustments and engine speed. The engine map in the engine module is three dimensional map that shows the variation of engine torque with respect to engine speed and gas pedal percentage. The rotating shaft of the engine connects the clutch module to the transmission.

5.2 Simulation Inputs

Simulation inputs are illustrated by a fishbone diagram in Figure 5.6:

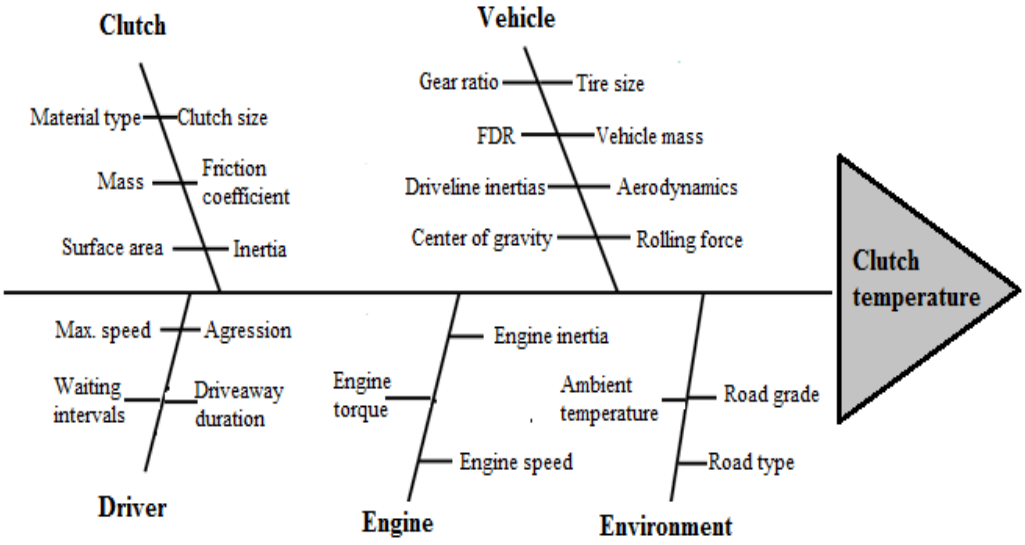

Figure 5.6 : Fishbone diagram for the simulation inputs and outputs.

5.3 Assumptions in Simulation

There were a number of assumtions made in the simulation, especially due to fact that the test is a driver dependent test. These assumtions are mentioned below:

a) The gas pedal inflection percentage flactuates around 80% in the simulation. The actual value is also close, but not exact.

b) The clutch housing's mass and surface area are a little larger than their actual values since there are additional components such as clutch release fork and release bearing in the clutch housing, which also absorb the heat energy.

c) The engine does not reach extreme speeds, which is also instructed to drivers prior to actual tests. This is achieved by the engine speed controller in the model.

5.4 Simulation and Test Results

The air temperature within the clutch housing was recorded at each step of the test and the final temperatures were analyzed. It was seen that all thermocouples inside the clutch housing measured the same air temperatures. The comparison of the simulation and the test results of the air temperatures within the clutch housing according to time is given in Figure 5.7.

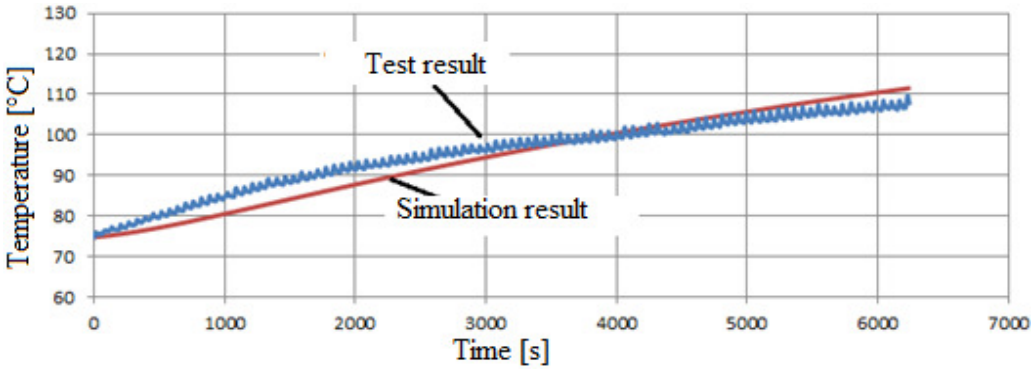

Figure 5.7 : Clutch housing temperature vs time – Vehicle 1.

Figure 5.8 shows the comparison of the test and simulation results for Vehicle 2.

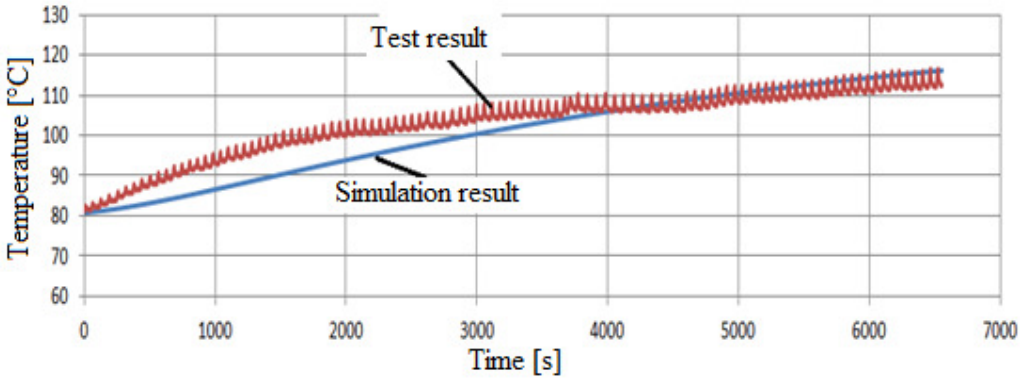

Figure 5.8 : Clutch housing temperature vs time – Vehicle 2.

The same comparison for Vehicle 3 is shown in Figure 5.9.

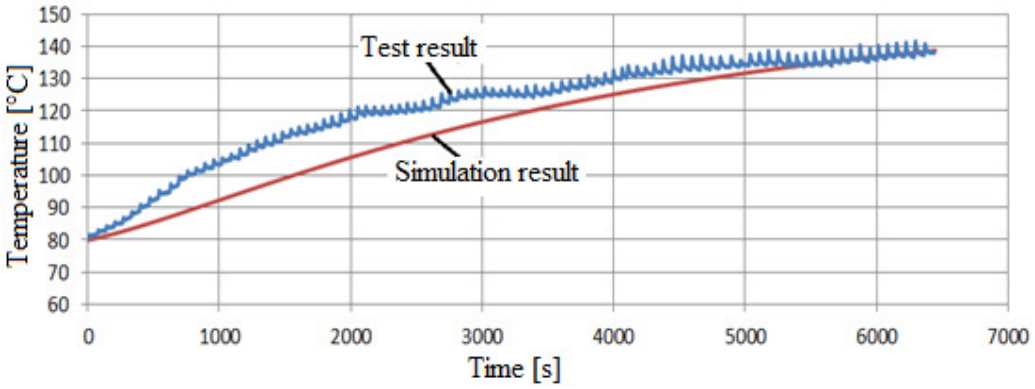

Figure 5.9 : Clutch housing temperature vs time – Vehicle 3.

The final air temperature values in the clutch housing for all vehicles are given in Table 5.1.

Table 5.1 : Test and simulation results comparison.

	Clutch housing final temperatures [°C]	
	Simulation	Test
Vehicle 1	111	108
Vehicle 2	112	113
Vehicle 3	138	138

6. DESIGN OF EXPERIMENT (DOE)

6.1 Setup

A full factorial DOE was performed on GT-SUITE to determine some of the most important factors affecting the clutch energies with their magnitutes. The main vehicle properties effecting the clutch heat dissipation and their number of levels were selected, keeping the other variables constant. As a result of selected factors and their number of levels in Table 6.1, total 432 simulations run in DOE.

Table 6.1 : Main factors and levels for DOE.

Factor	Minimum	Median	Maximum	# of Levels
First gear ratio	12.8	13.8	14.8	3
FDR	2.7	2.85	3	3
GTM [kg]	40000		45000	2
Grade [%]	10	-	12	2
Tyre size [mm]	458	492	526	3
Ambient temperature [°C]	10	-	30	2
Max. engine torque [Nm]	2040	-	2240	2

6.2 Results for DOE

6.2.1 Goodness of fit

Coefficient of determination (R^2) and adjusted coefficient of determination are found 96.7% and 96.24%, respectively. The results for the goodness of fit are given in Figure 6.1.

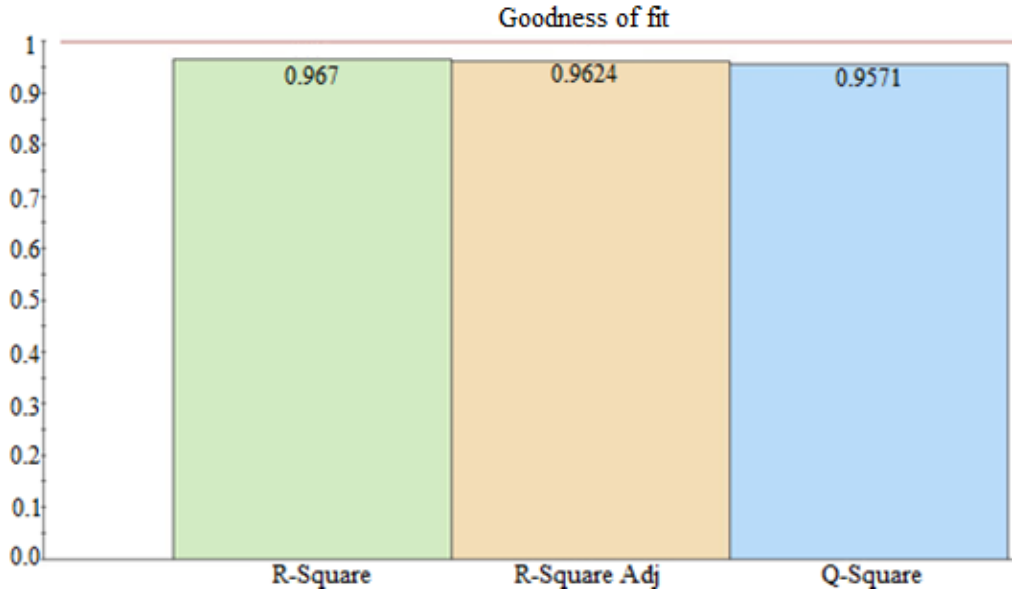

Figure 6.1 : Accuracy of DOE.

6.2.2 Effects pareto for clutch housing temperature

Figure 6.2 mentions the pareto chart which shows the magnitute and the importance of an effect. It can be understood that the transmission ratio effects the energy dissipation in the clutch the most, followed by the tire size, FDR, vehicle mass, engine torque, slope of the road and ambient temperature, respectively.

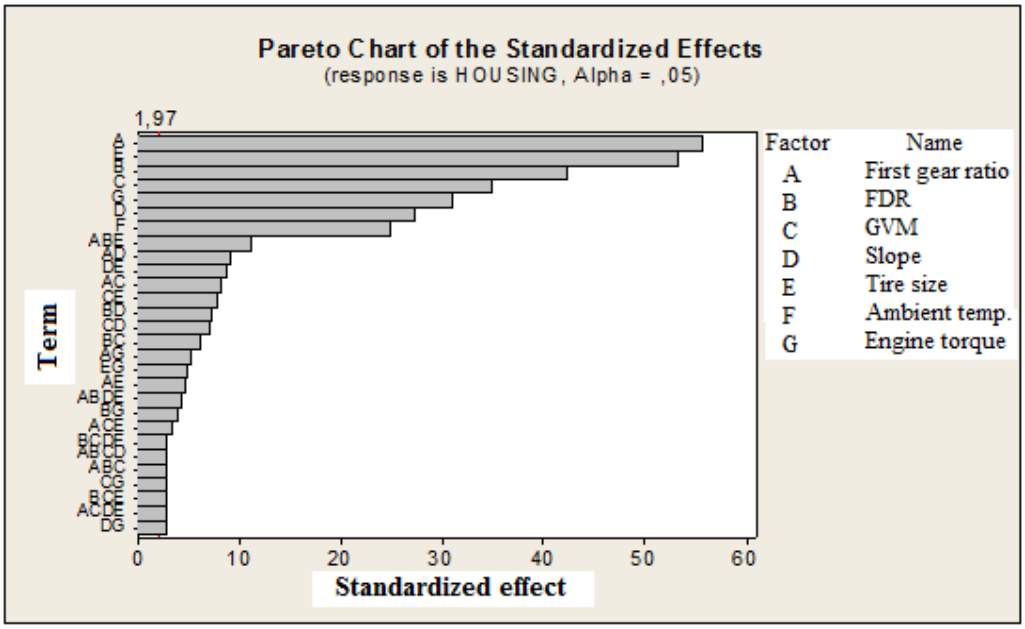

Figure 6.2 : Pareto chart for the clutch housing temperature.

6.2.3 Main effects plot for clutch housing temperature

The main effects plot shows how the clutch housing temperature changes with respect to each factor. It can be seen from Figure 6.3 that the contribution of the ambient temperature has the least effect on the clutch housing temperatures.

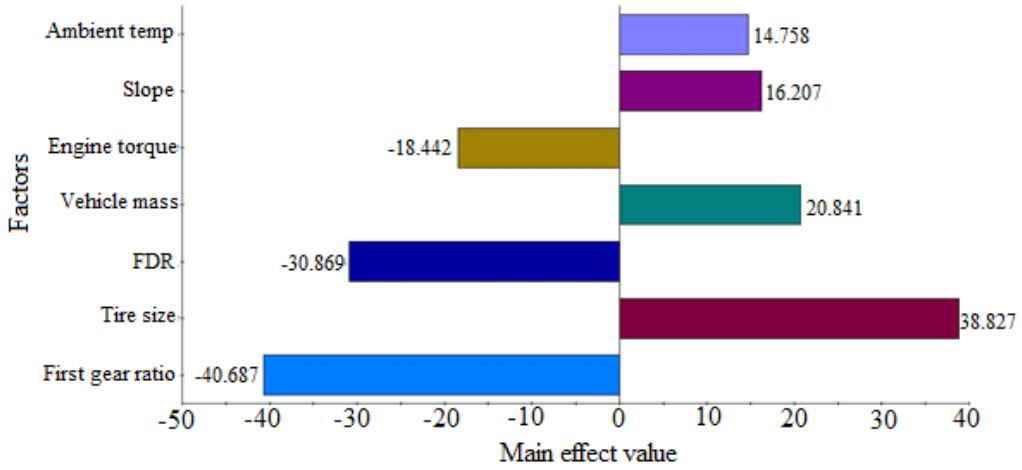

Figure 6.3 : Main effects plot for the clutch housing temperature.

6.2.4 Interaction plot for clutch housing temperature

The combined effects of the parameters on the clutch housing temperatures are seen in the interaction plot in Figure 6.4.

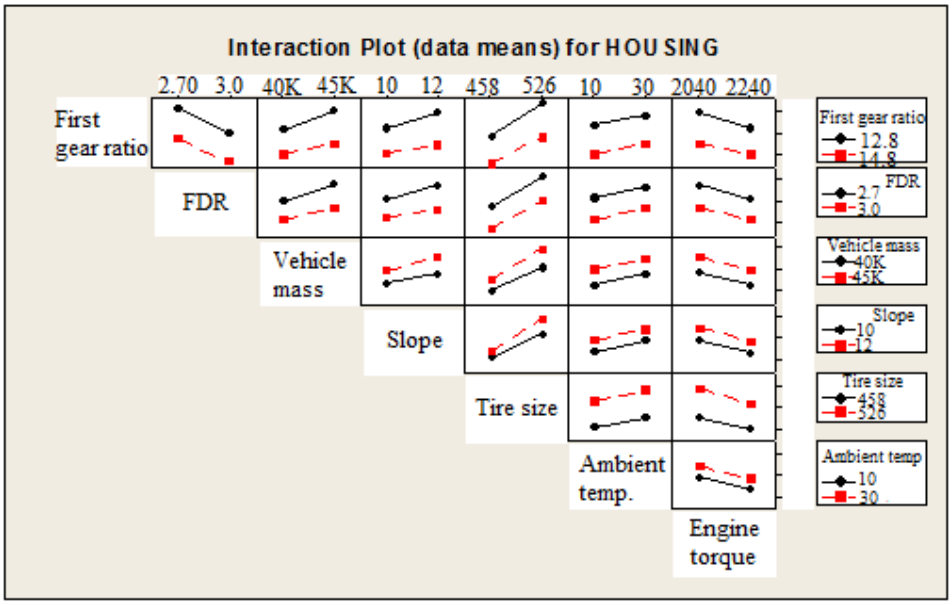

Figure 6.4 : Interaction plot for the clutch housing temperature.

6.2.5 The equation for the clutch housing temperature by DOE

DOE gives an equation for the clutch housing temperature as a function of the factors. The difference in the results between the DOE equation and the simulation is less than 5% for a certain range of the factor values. The results can be seen in Table 6.2.

Table 6.2 : DOE and simulation results for clutch housing temperatures.

Factor	1st	2nd	3rd
Transmission ratio	13	13.2	14
FDR	2.75	2.8	2.7
GVM [kg]	41000	42000	45000
Grade [%]	11	11	12
Tire size [mm]	480	490	510
Ambient temperature [°C]	15	18	25
Max. engine torque [Nm]	2100	2150	2200
DOE result [°C]	156.08	154.68	189.2
Simulation result [°C]	147.7	144.1	178.2

7. DISCUSSION AND CONCLUSION

7.1 Discussion

In this thesis, the simulation of the clutch hill start test has been established. A complete vehicle structure and a driver profile have been modeled. The test procedure is followed thanks to the driver profile in the simulation. Clutch housing temperatures have been obtained as an output of the simulation. The integrity of the simulation has been validated with three physical vehicle tests. The deviation between the actual test and simulation results are as low as 2%. In addition, a DOE has been performed to see the impacts of selected factors on the heat energy dissipation and clutch housing temperatures. These effects were tabulated with their magnitudes and the most critical factors have been found.

432 simulations run in DOE and the results have an accuracy rate of 94%. The essential factors playing role in temperature rising of the clutch housing have been determined with their degree of magnitudes. This means that each parameter has a unique effect in the results. For instance, reducing the first gear ratio will influence the clutch temperatures more than reducing the final drive ratio even if the percent of the change is same. Another example of optimizing the clutch temperatures is that since the ambient temperature effect has been evaluated, optimizing the clutch temperatures and even fuel economy become possible for the vehicles shipped to the cold regions. These vehicles could be equipped with a smaller final drive ratio. In this situation, the clutch will heat up more, however, due to the ambient temperature, it will cool down. Eventually, the vehicle can consume less fuel as the clutch temperature remains in the safe range. Yet another benefit of the model is that making a modicification in the transmission is very difficult unless the OEM is able to manufacture its own. The transmission manufacturers sell the same transmission to plenty of the OEM for reducing the product complexity. Hence, optimizing the transmission gear ratios might be impossible. Knowing that each parameter influences the clutch life at a different rate, the properties of different driver

properties such as the final drive ratio or tire radius can be modified, considering that transmission gear ratios are constant.

The model takes the variation of the friction coefficient of the clutch disc linings with respect to temperature into consideration. The friction coefficient tends to be constant at a narrow range of temperature values. However, it decreases drastically as the temperature continues to increase. This means that the heat in the clutch due to the friction increases exponentially at each step of the test as the temperature keeps rising, which can burn the clutch easily. Considering this in the simulation is crucial for obtaining consistent results. In addition, it enables us to compare different types of clutch linings made of organic and ceramic, for instance.

According to the test procedure, each test is performed with a normal driver aggression, meaning that the driver prevents any abrubt clutch and gas pedal adjustments. This driver profile has been modeled in the simulation. As an input of the tool, the aggression of the driver can also be modified with respect to the different test conditions. For instance, a sport or a professional driver can be created. In any case, the torque flow rate and the clutch housing temperatures will be different.

7.2 Conclusion

Technically, the tool aims to investigate the clutch temperatures during the clutch hill start test, which helps predict risky cases for the clutch as well as product validation and optimization. In addition to driveline optimization, clutch properties such as mass, surface area, inertia and friction material can be improved.

It is quite simple to apply the model to passenger cars as well, provided the clutch thermal section needs to be correlated according to the passenger cars' clutch housing mass and surface area properties.

Finally, the model provides a tool to save money and time, which are spent for the tests.

REFERENCES

[1] **Albers, A., Meid M., and Ott, S.** (2010). Avoiding of Clutch Excited Judder Using an Active Clamping Force Control. *International Conference on Noise and Vibration Engineering.*, Karlsruhe Institute of Technology (KIT), Germany, September 22.

[2] **Oday, I. A., and Schlattmann, J.** (2012). Finite Element Analysis for Grooved Dry Friction Clutch, *Advances in Mechanical Engineering and its Applications.*, Institute of Laser and System Technologies, Technical University Hamburg, Germany.

[3] **Nunney, M. J.** (2006). *Light and Heavy Vehicle Technology*., Vol. 4, pp. 265.

[4] **Kimmig, K. L. S.** (1998). The Self-Adjusting Clutch SAC of the 2nd Generation. 6*th LuK Symposium.,* LuK GmbH, Germany.

[5] **Maekawa, K., Obikawa, T., and Yamane, Y.** (2003). Mechanical Design., Vol. 2, pp. 192.

[6] **Szikrai, S.** (2012). Clutch Disc Design. *LuK Product Training.,* LuK GmbH, Buehl-Germany, July 16-19.

[7] **Albert, V., and Hillier, W.** (1991). *Fundamentals of Motor Vehicle Technology*., Vol. 4, pp. 214.

[8] *Clutch Systems, For Passenger Cars up to 800Nm.*

<http://www.zf.com/media/media/en/document/corporate_2/downloads_1/flyer_and_brochures/cars_flyer/kupplungssystemefrpkwbis800nm.pdf>, date retrieved 10.08.2014.

[9] *An Introduction to Clutch Technology For Passenger Cars.*

<http://www.luk.de/content.luk.de/en/services/mediathek/library/library-detail-language.jsp?id=3550720>, date retrieved 10.08.2014.

[10] Performance Race – Clutches and Flywheels., *Exedy Racing Clutch Brochure*, April 2013.

[11] *An Explanation of Principal Clutch Types.*

<http://www.valeoservice.com/data/master/webfile/12799550454E7C37A1AE46F.pdf?rnd=602>, date retrieved 15.08.2014.

[12] Sport Clutches and Flywheels., *Exedy Racing Clutch Brochure*, June 2010.

[13] **Garrett, T. K., Steeds, W., and Newton, N.** (2001). *Motor Vehicle.*, Butterworth-Heinemann, London.

[14] *Powertrain Components and Systems for Commercial Vehicles.*

<http://www.zf.com/media/media/document/corporate_2/downloads_1/flyer_and_brochures/powertrain_and_suspension_components/06_Nkw_Antriebsstrang_2008_E.pdf>, date retrieved 22.08.2014.

[15] Clutch Disc Assembly Training., *Valeo Transmissions Technical Institute*, France, June 2012.

[16] **Buer, M.** (2009). Die Kupplungsscheibe im Antriebsstrang*., Technical Document, ZF Friedrichschafen.*

[17] **Felger, R., Spandern, C.** (2006). Innovative Clutch Facing Materials*., 8th LuK Symposium.,* LuK GmbH, Germany.

[18] *Experiencing Dynamics – Reliably CV Powertrain Modules.*

<http://www.zf.com/media/media/en/document/corporate_2/downloads_1/flyer_and_brochures/cars_flyer/antriebskomponentenundsystemefrnutzfahrzeuge.pdf>, date retrieved 20.09.2014.

[19] **Maucher, P.** Clutch chatter, Kupplungsrupfen Möglichkeiten zur Vermeidung*., 8th LuK Symposium.,* LuK GmbH, Germany.

[20] **Hiriyannaiah, A.** Lecture Notes, For 6th semester., *BE Mechanical PES Institute of Technology*, India.

[21] **Randazzo, L.** (2012). Clutch Cover and SAC *Training.,* LuK GmbH, Buehl-Germany, July 16-19.

[22] **Shaver, R.** (1997). Manual Transmission Clutch Systems, *SAE International,* pp 34.

[23] *Introduction to truck service manual.*

<http://www.valeoserviceusa.com/sites/default/files/techdoc/Truck%20Service%20Manual%20-%20Clutches.pdf>, date retrieved 05.10.2014

[24] *Trade of Heavy Vehicle Mechanic.*

<http://local.ecollege.ie/Content/APPRENTICE/liu/hvm_notes/M3U2.pdf> date retrieved 05.10.2014

[25] Flywheel Assembly Training., *Valeo Transmissions Technical Institute*, France, June 2012.

[26] *Clutch servo installation manual*

<http://www.wabcoindiaportal.com/ser_manual/clutch%20servo_installation%20guideline_rev5.pdf> date retrieved 06.10.2014

[27] **Gopinath, K., Mayuram, M.** Lecture Notes, Machine Design II.., *Indian Institute of Technology Madras, India.*

[28] **Liu, Y., Qin, D., Jiang, H., Liu, C., Zhang, Y.** (2010). Clutch torque formulation and calibration for dry dual clutch transmissions., *Mrchanism and Machine Theory,* Vol. 46, pp. 218-227.

[29] **Abdullah, O.I., Schlattmann, J.** (2012). Effect of Band Contact on the Temperature Distribution for Dry Friction Clutch., *World Academy of Science*, Engineering and Technology, Vol. 6, No. 9.

[30] **Abdullah, O.I., Schlattmann, J.** (2013). Contact Analysis of a Dry Friction Clutch System., *ISRN Mechanical Engineering,* Department of System Technology and Mechanical Design Methodology, Hamburg University of Technology, Germany.

[31] **Watson, M., Byington, C., Edwards, D., Amin, S.** (2004). Dynamic Modeling and Wear-Based Remaining Useful Life Prediction of High Power Clutch Systems., STLE Tribology Transactions, Vol. 48, pp. 208-217.

[32] **Hebbale, V. K., Samie, F.** (2012). Thermal model for dry dual clutch transmissions, *United States Patent*, No: *20120290249 dated 15.11.2012*

CURRICULUM VITAE

Name Surname: Cem Erbaş

Place and Date of Birth: Istanbul - 1985

E-Mail: cemerbas@gmail.com

B.Sc.: Mechanical Engineering at Kocaeli University

Professional Experience and Rewards: February 2012 – Present, Product Development Engineer for Clutch Systems, Ford Motor Company

Powertrain Engineering Award for Engineering Excellence by Ford of Europe "Simulation of the clutch hill start test for heavy commercial vehicles"